ISSN 0429-8284

Whole Number 213

e-Front runners

FUJI ELECTRIC REVIEW

2

2006 VOL.52

Semiconductors

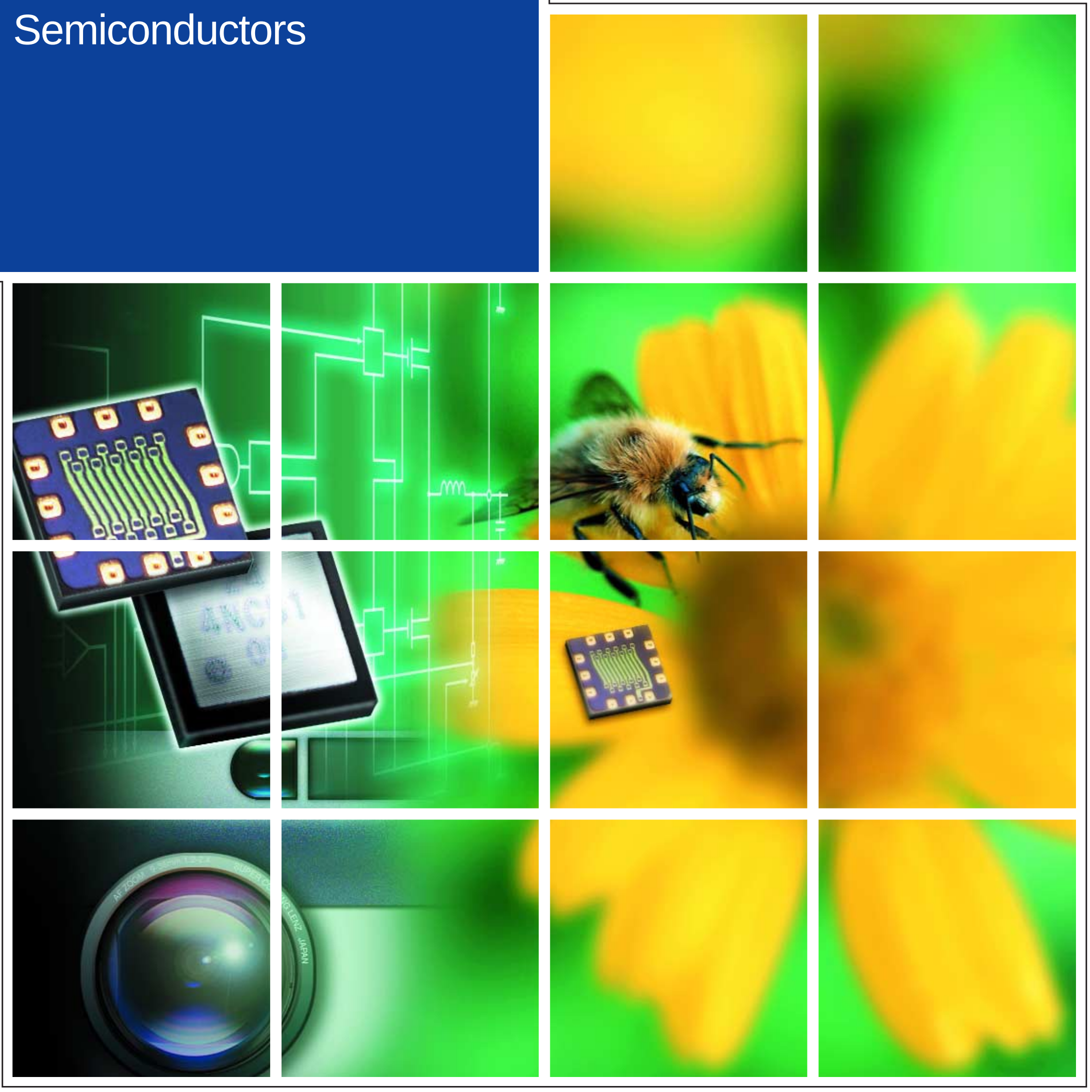

Fuji Electric Group

e-Front runners

Quality is our message

Effective for Energy Savings in an AC-DC Converter

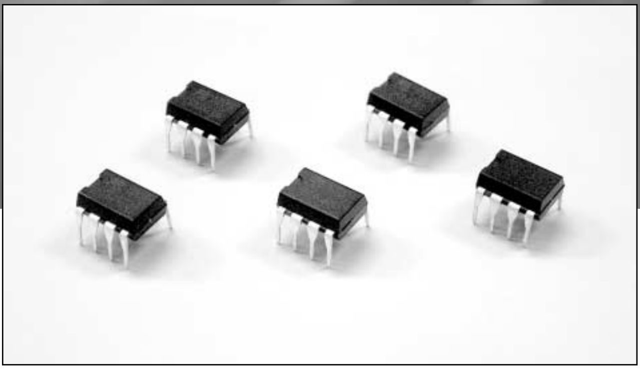

Features

- Built-in 500 V high-voltage JFET (junction field-effect transistor). Low switching frequency during light load operation. Power supply input power of 60 to 140 mW realized during unloaded operation. (80 to 264 V AC, unloaded operation at approximately 1 kHz)
- Quasi-resonant control. Low noise and high efficiency at maximum 130 kHz operation.
- Auto-restart type overload protection (Repeated operation of 0.2 s ON / 1.5 s OFF)
- Excellent MOSFET driving capability (Output stage: High-side 17 Ω, Low-side 3.5 Ω). Can be used in a 200 W quasi-resonant power supply.
- Wide range of VCC operating voltages: 10 to 28 V. Auxiliary winding does not require a series regulator.
- Soft-start function (1 ms fixed)
- VCC pin provided with 28 V, with overvoltage timer latch protection.

Block diagram

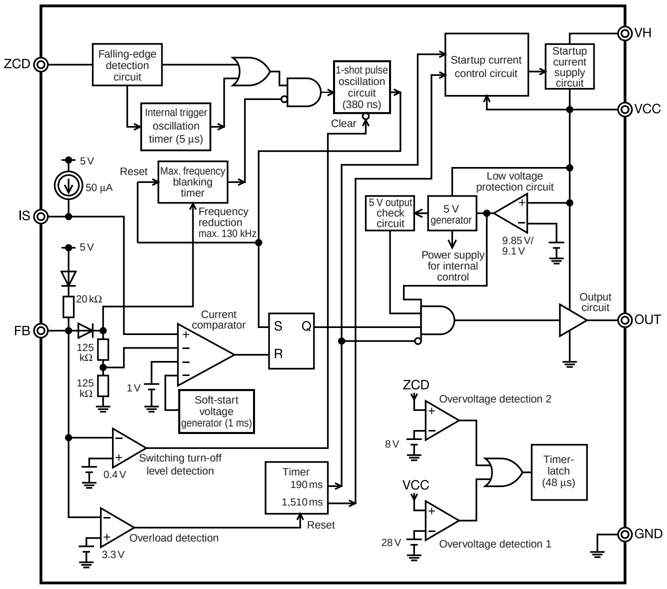

Example application circuit

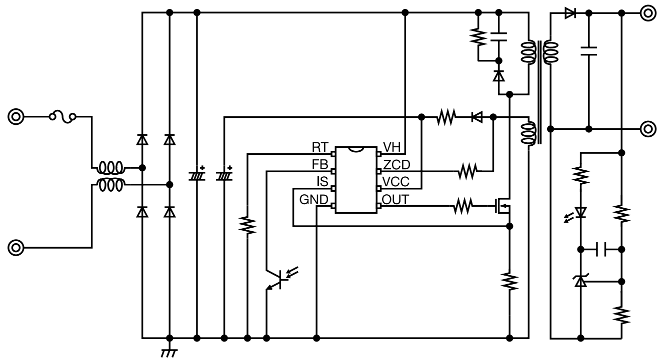

Fuji Electric's Quasi-resonant Controller IC

FA5531

FUJI ELECTRIC
REVIEW

2

2006 VOL.52

Semiconductors

CONTENTS

Cover photo:

Portable electronic equipment such as digital cameras, digital video cameras, and cellular phones have advanced year-by-year toward smaller size and greater multi-functionality. Smaller size and lower power consumption are also required in the DC-DC converters used to control the power supplies in this type of equipment.

Responding to these market requests, Fuji Electric has developed and commercialized micro DC-DC converters equipped with an integrated control IC and inductor. Realizing the compact dimensions of 3.5 mm × 3.5 mm, and having a maximum thickness of 1 mm, these new products will facilitate the miniaturization of portable electronic equipment to much smaller sizes than in the past.

The cover photo contrasts a micro DC-DC converter, the front of which shows an inductor made of a ferrite base, with a honeybee to conceptually illustrate the compact size of the micro DC-DC converter.

Fuji Electric Holdings Co., Ltd. Head Office : No.11-2, Osaki 1-chome, Shinagawa-ku, Tokyo 141-0032, Japan
http://www.fujielectric.co.jp/eng/company/tech/index.html

Fuji Electric's Semiconductors: Current Status and Future Outlook

Tatsuhiko Fujihira
Hirokazu Kaneda
Shu-ichiro Kuneta

1. Introduction

Influenced by economic growth and an increasing population, by 2025 the global consumption of primary energy will be 1.5 times that consumed in 2001, and will be the equivalent of 15.7 billion tons of oil. As a result, carbon dioxide (CO_2) emissions are predicted to rise to 1.5 times that of 2001, or to 37.1 billion tons. Unless the trend toward increasing atmospheric concentrations of CO_2 and other greenhouse gases is slowed, it has been reported that by the end of the 21st century there will be a worldwide average increase in land temperature of 1.4 to 5.8°C and sea levels will rise by 9 to 88 cm due to the greenhouse effect. The effects of global warming are not limited to a rise in sea levels, and wide-ranging large-scale effects including damage to the ecosystem, severe droughts, adverse impact on food production, frequent flooding and storm surges, increased incidence of tropical diseases, and the like, have been predicted and reported.

Improving industrial productivity is essential for raising living standards and for economic development, and among the types of energy consumed, an especially large increase in the consumption of electrical power is forecasted. As shown in Fig. 1, by 2025, the global consumption of electrical power is forecasted to increase to 23 trillion kWh, approximately 1.7 times that consumed in 2001(1). From the perspective of people involved in the power semiconductor business, one sector of the power electronics field that targets the effective use of electric power energy, the above figures underscore the importance of their mission to strike a balance between global improvements to the standard of living and economic development on one hand, and protection of the global environment on the other.

Fig.1 Forecast of global electric power consumption(1)

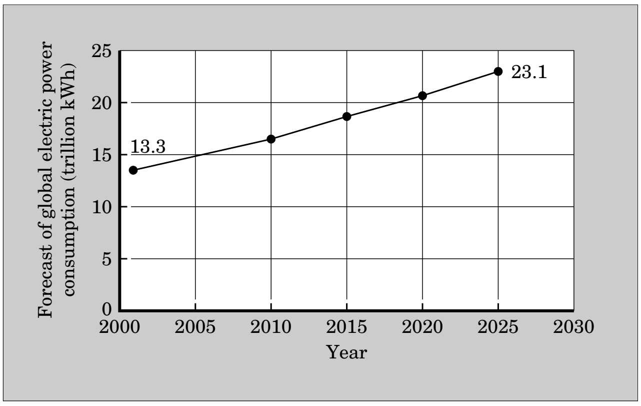

For power semiconductors to contribute to this mission, the efficiency of electric power utilization in power electronic equipment must be improved, and the savings of natural resources (miniaturization) and expanded range of use (lower cost and wider range of applications) must exhibit positive effects. Specifically, performance improvements to power semiconductors and improved control and sensing functions must contribute to advances in performance, smaller size, higher reliability and lower cost, and must also expand the power semiconductor product lineup and its range of applications.

This paper discusses the current status and future outlook for Fuji Electric's representative semiconductor products of power modules, power discretes and power ICs.

2. Power Modules

High-power semiconductor devices used for electric power conversion and other applications in industrial machinery and robots, air conditioner compressors, semiconductor manufacturing equipment, motor drives of automobiles and hybrid electric vehicles, welders and UPS (uninterruptible power supplies), medical equipment, and the like, are supplied mainly as power modules. From the commercialization of IGBT (insulated gate bipolar transistor) products in 1988 through the present, due to their excellent performance and controllability, IGBTs have evolved to become the type of transistors used most commonly in power modules.

Figure 2 shows the historical changes in performance and technology of Fuji Electric's IGBT modules, using the 1,200 V series as an example. At present, the latest generation is the 5th generation U-series released in 2002. By using an FS (field stop) structure for the device, and using a trench-gate structure for the gate, dramatically lower loss and higher rugged-

Fig.2 Changes in performance and technology of Fuji Electric's IGBT modules

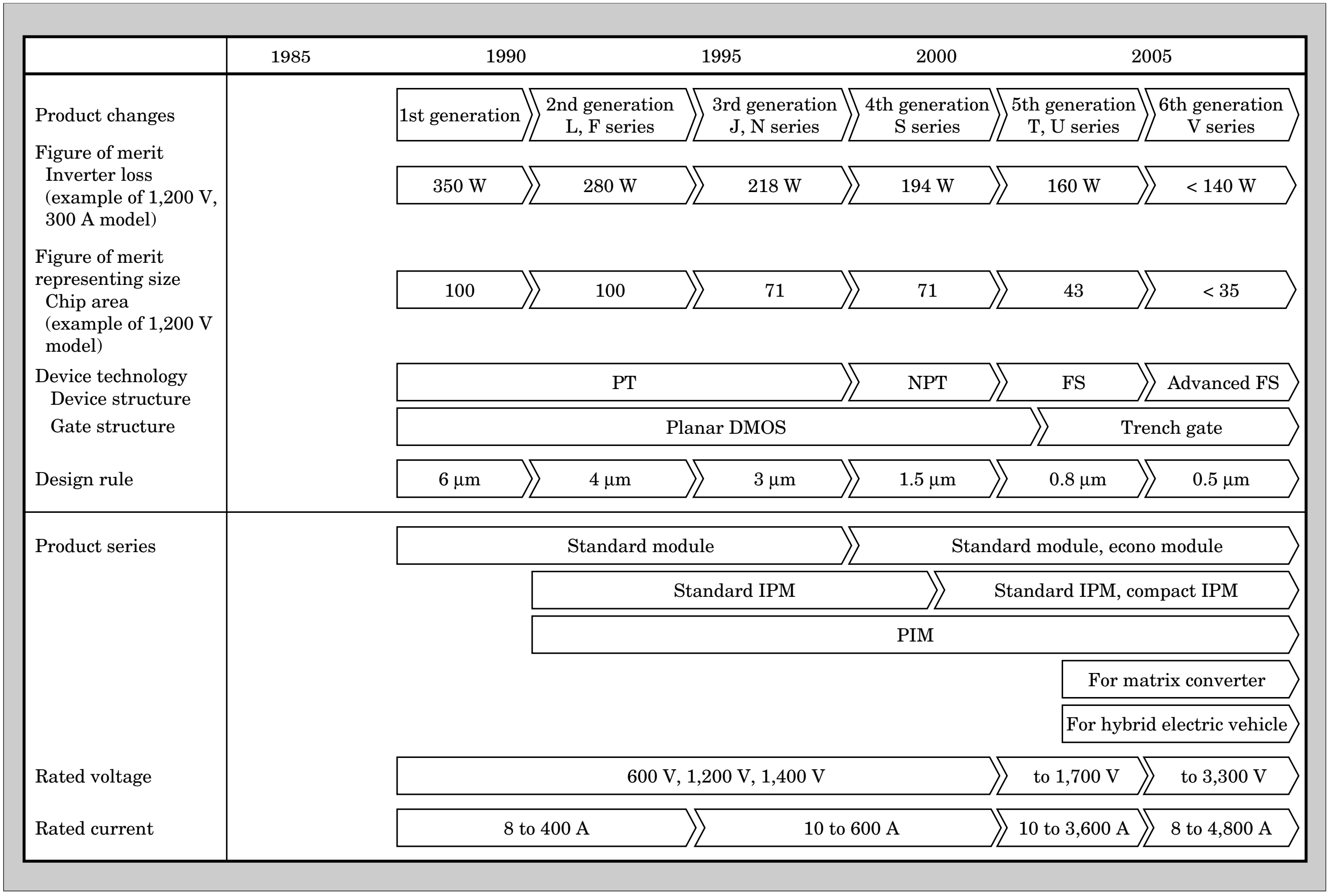

ness have both been realized, and by using an anode structure known as a SAS (shallow anode structure) that suppresses carrier injection, the performance of the FWD (free wheeling diode) has also been improved. In the example of the 1,200 V series, approximately 20 % lower loss and approximately 40 % smaller chip area as compared to the 4th generation IGBT modules have been realized in the case of 6 kHz inverter operation. In the upcoming 6th generation V-series, additional improvements to the device structure (advanced FS structure) and an improved gate structure are planned to further reduce power loss and shrink the chip size, and FWD improvements are also planned at this time. 1,200 V models of the V-series are slated for release in fiscal year 2006, and 600 V models for fiscal year 2007.

As its IGBT module lineup, Fuji Electric first began supplying a standard module series, but then with the 2nd generation of modules, added an IPM (intelligent power module) and PIM (power integrated module) series and with the 3rd generation dramatically increased the number of types of models, and then with the 4th generation, added a small-size low-cost EconoPACK*1 series. With the 5th generation, Fuji Electric added a 1,700 V series of modules, expanded the large-current series to 3,600 A, started to provide custom designed IGBT modules for hybrid vehicles, and advanced the commercialization of reverse-blocking IGBT modules for matrix converter use. Fuji Electric is committed to continuing to expand the voltage and current range of high-power IGBT modules, to achieve even smaller size and lower cost in low-power IGBT modules, and to actively support new applications.

When considering the future of power modules, the most important issue is when to make the transition from silicon (Si) devices such as IGBTs to compound semiconductor devices such as silicon carbide (SiC) devices. Fuji Electric estimates that the transition of power modules to SiC technology will occur at the time of the 7th or 8th generation. SiC wafer technology has made steady progress in reducing defect density and developing larger diameter wafers. By the time when the 7th generation is released in 2009 or 2010, a killer defect density of less than 10 cm^{-2} may be achieved for the 4-inch wafers needed to mass-produce 5 mm chips. However, the cost of SiC wafers presents an extremely large challenge. Even with the assumption of other improvements such as the realization of smaller package sizes as a result of the effective utilization of the smaller chip size, and the realization a large increase in the maximum rated junction temperature, the price

---

∗1: EconoPACK is a trade mark of Eupec GmbH. Warstein.

per unit area of SiC wafers must be reduced to about 1/30th of their present cost in order for them to be a viable substitute for IGBT chips, and the present cost reduction trend is not on track to meet this requirement. We look forward to further technical innovation and effort by the SiC wafer manufacturers. Power device manufacturers must concentrate on researching SiC processes and devices, while at the same time hedging their risk by continuing to improve the performance of Si devices. However, with the 6th generation of devices, IGBT performance improvements will approach their limit, and a radically innovative device structure will be needed to realize the 7th generation devices. Efforts must also focus on research into new types of Si devices such as MOS (metal oxide semiconductor) gate thyristors, and research into package technologies(9), (10) capable of utilizing the Si devices at higher current densities.

3. Power Discretes

Medium-power semiconductor devices used in switching-mode power supplies, UPS for IT (information technology) equipment, automotive-use drivers for motors, relays or solenoids, and the like, are supplied mainly as power discrete products. Because of their excellent high-frequency performance and drivability, power MOSFETs (MOS field effect transistors) are the most commonly used type of discrete transistors, and also from the perspective of high-frequency performance, LLDs (low loss diodes) are the mainstream diode for high-voltage applications, and similarly, SBDs (Schottky barrier diodes) are used for low-voltage applications.

This chapter discusses the present status and future outlook for power MOSFETs, LLDs and SBDs.

3.1 Power MOSFETs

Figure 3 shows the historical changes in performance and technology of Fuji Electric's power MOS FETs. Fuji Electric's 600 V series is shown as a representative example of a high-voltage series for use in switching-mode power supplies, and the 60 V series is shown as a representative example of a low-voltage series for automobile-use.

The flagship of the high-voltage series is presently the 3rd generation SuperFAP-G series released in 2001. With the two independent technologies of a quasi-plane junction and an optimized guard ring, this SuperFAP-G series realizes high performance that approaches 10 % to the theoretical limit for Si. In the example of the 600 V series, an approximate 60 % reduction in the figure of merit $R_{on}Q_{gd}$ indicating low-loss performance was achieved compared to the 2nd generation products, and a smaller size corresponding to an approximate 40 % reduction in the figure of merit $R_{on}A$ representing chip size and assurance of repetitive avalanche ruggedness at elevated temperature were achieved at simultaneously. For the upcoming 4th generation, the use of super-junction technology to realize even lower loss and smaller size is being studied.

In the low-voltage series, the shipment of samples of the 5th generation FAP-T2 series (2nd generation of trench MOSFETs) started in 2004. With a trench gate structure and improved quasi-plane junction technology, the 60 V series achieves an approximate 30 % reduction in $R_{on}Q_{gd}$ and an approximate 20 % reduction in $R_{on}A$ compared to the 4th generation products, while maintaining the high reliability (high avalanche

Fig.3 Changes in performance and technology of Fuji Electric's power MOSFET modules

	1985	1990	1995	2000	2005	
600 V product changes	1st generation (FAP-1, FAP-2 series)	2nd generation (FAP-2A, FAP-2S series)	3rd generation (SuperFAP-G series)	4th generation		
$R_{on}Q_{gd}$	20 Ω·nC	15 Ω·nC	5.5 Ω·nC	3 Ω·nC		
$R_{on}A$	130 m$\Omega\cdot$cm^2	125 m$\Omega\cdot$cm^2	76 m$\Omega\cdot$cm^2	24 m$\Omega\cdot$cm^2		
Device technology	Planar DMOS		Quasi-plane junction DMOS	Super-junction		
60 V product changes	1st generation (FAP-1 series)	2nd generation (FAP-3A series)	3rd generation (FAP-3B series)	4th generation (FAP-T1 series)	5th generation (FAP-T2 series)	6th generation (FAP-T3 series)
$R_{on}Q_{gd}$	800 mΩ·nC	540 mΩ·nC	260 mΩ·nC	175 mΩ·nC	125 mΩ·nC	90 mΩ·nC
$R_{on}A$	3.5 m$\Omega\cdot$cm^2	2.3 m$\Omega\cdot$cm^2	1.4 m$\Omega\cdot$cm^2	0.8 m$\Omega\cdot$cm^2	0.65 m$\Omega\cdot$cm^2	0.5 m$\Omega\cdot$cm^2
Device technology	Planar DMOS		Quasi-plane junction DMOS	Quasi-plane junction trench		

Fig.4 Fuji Electric's diode (LLD and SBD) performance improvements and expansion of product lineup

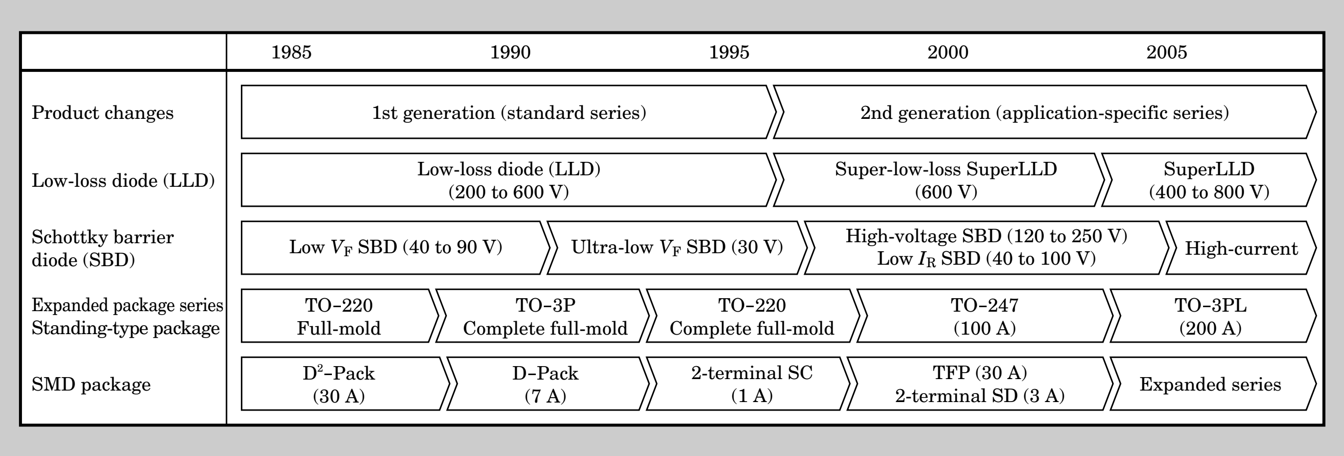

ruggedness, high short-circuit withstand capability, high breakdown voltage of the gate, high power-cycling capability) of the 4th generation. In the upcoming 6th generation, we plan to further optimize the trench gate structure and the quasi-plane junction technology to realize smaller design rules, while maintaining the trends towards improved performance and smaller size.

3.2 LLDs and SBDs

Figure 4 shows historical performance improvements and expansion of the series of Fuji Electric's LLDs and SBDs. LLDs are used primarily in the secondary-side rectification of switching-mode power supplies and in power-factor control circuits, and the 200 to 600 V standard series and the 600 V SuperLLD series are presently the flagship models. The SuperLLD series contains a low switching loss series for use with continuous conduction mode PFC (power-factor control) and a low conduction loss series for use with discontinuous conduction mode PFC. In the future, we plan to expand the rated current and voltage ranges of our LLDs.

SBDs are used primarily in DC-DC converters and in the secondary-side rectification of switching-mode power supplies, and the 120 to 250 V rated high-voltage SBDs and the 40 to 100 V rated low-reverse-leakage-current (low I_R) SBDs are presently the flagship models. The high-voltage SBDs use newly developed barrier metals to realize higher voltage and, at the same time, reduced leakage current and lower switching noise. By using these high-voltage SBDs in applications in which 200 to 400 V LLDs had been used previously, lower loss and lower noise can be achieved. As expected, by using newly developed barrier metals, low-I_R SBDs can reduce leakage current to approximately one-tenth that of conventional SBDs, and can be used at junction temperatures of up to 150°C, and are therefore especially effective in applications where the heat radiation is poor such as in AC adapters. In the future, we plan to increase the current capacity of these products and to expand the lineup of available packages.

4. Power ICs

4.1 Power ICs for automotive-use

Fuji Electric supplies many series of power ICs. Automotive-use power ICs include single-chip and hybrid igniters for ignition, IPS (intelligent power switches) for driving the solenoid valves of an electronic transmission controller, smart power MOSFETs for driving solenoid valves in ABS (antilock brake systems) and ESC (electronic stability control) systems and for driving lamps, and integrated power ICs for integrating multiple I/O channels in ECU (electronic control units).

4.2 Power ICs for power management systems and IT equipment

As power ICs for power management systems of IT equipment, Fuji Electric is focusing on power IC for power systems (hereafter referred to as power supply ICs). Figure 5 shows the historical changes in performance and technology of Fuji Electric's power supply ICs. Fuji Electric's latest generation of power supply ICs is its 4th generation 0.6 µm CDMOS (complimentary double diffused MOS). With an optimized structure and advanced design rule, the lateral DMOS achieves an approximate 17 % improvement in $R_{on}Q_{gd}$ and an approximate 25 % improvement in $R_{on}A$ compared to the 3rd generation products. In the upcoming 5th generation, we plan to transition to a CTMOS (complementary trench lateral power MOS) device that contains a TLPM (trench lateral power MOS) integrated into its output stage, and expect an additional approximate 40 % improvement in $R_{on}Q_{gd}$ and approximate 67 % improvement in $R_{on}A$. Power supply ICs are either for AC-DC use or for DC-DC use. AC-DC power supply ICs include AC-DC driver ICs, single-chip power ICs with an integrated high-voltage output power MOSFET, and M-power series for high-current

Fig.5 Changes in performance and technology of Fuji Electric's power ICs for power management systems and IT equipment and PDP driver ICs

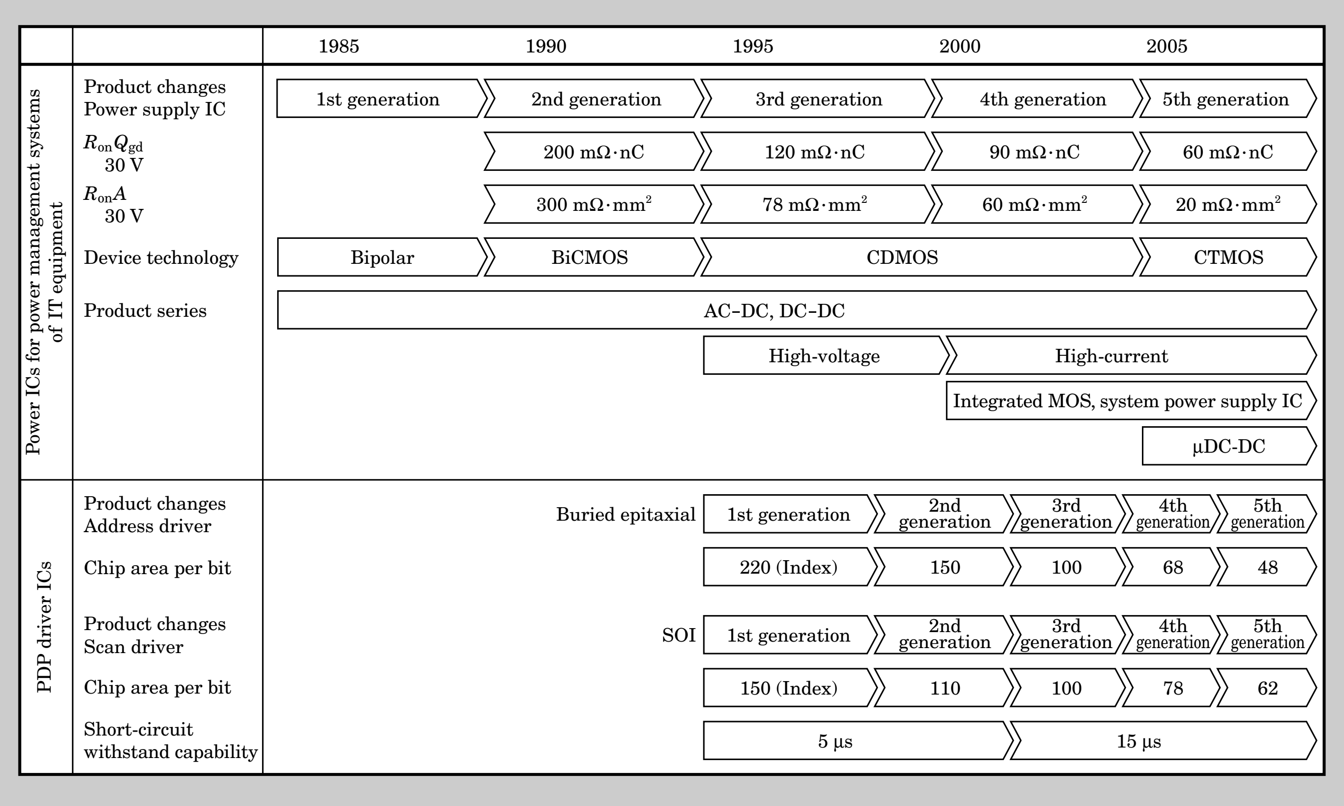

Fig.6 Fuji Electric's μDC-DC (micro DC-DC converter) that will contribute to the smaller size and lighter weight of portable electronic equipment

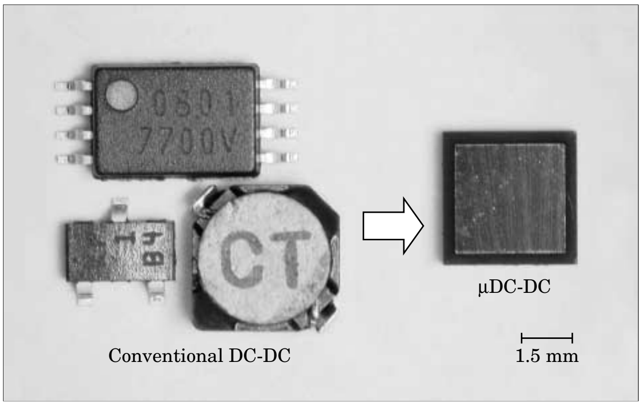

and high-efficiency power supplies. DC-DC power supply ICs include DC-DC power supply ICs with and without integrated power MOSFETs, system power supply ICs, and micro DC-DC converters. Among these devices, the micro DC-DC converter is a new product that uses Fuji Electric's proprietary technology and was just released at the end of 2004. As shown in Fig. 6, the micro DC-DC converter integrates the three components of a conventional power supply IC, a power MOSFET and an inductor into a single chip, thereby realizing a large reduction in the mounting area required on a printed circuit board. The micro DC-DC converter is especially effective in achieving smaller size and lighter weight in portable electronic equipment. This is one of the products that Fuji Electric intends to promote the most.

4.3 Drivers for plasma TV

The increase in demand for plasma TVs has resulted in a recent sudden increase in shipments of PDP (plasma display panel) drivers. There are two types of PDP drivers, scan drivers that drive the horizontal direction and address drivers that drive the vertical direction, and Fuji Electric has been supplying both types since the inception of the PDP era. Figure 5 shows the historical changes in performance and technology of Fuji Electric's PDP drivers. Address drivers began to be mass-produced with the 4th generation in 2005. By transitioning to 0.6 μm CD MOS technology and optimizing the lateral DMOS, these 4th generation address drivers achieve an approximate 32 % improvement in chip-area-per-output-bit as compared to 3rd generation products, and make it possible to support 192-bit driver ICs. In the upcoming 5th generation address drivers, further shrinkage of the design rules and device optimization to realize an additional improvement of approximately 30 % in the chip-area-per-output-bit, and the application of LVDS (low voltage differential signal) technology to increase the high-speed data transmission capability, are expected to provide the capability for supporting 256-bit driver ICs. 3rd generation scan drivers are presently being supplied. These 3rd generation scan drivers feature an improved output IGBT that realizes a 10 % reduction in the chip-area-per-output-bit and smart-gate control technology that has been developed to increase the short-circuit withstand capability to approximately three times its former value, and contribute to the realization of high quality plasma TVs. In the 4th generation scan drivers slated to begin mass production in fiscal year 2005, and the application of smart-gate control technology to the upper IGBT results in increased current density in the upper IGBT and reduces the chip-area-per-output-bit by an additional 22 %.

5. Transition to Lead-free Technology

In order to protect the global environment, efforts are underway to eliminate certain hazardous substances from the environment. For semiconductor products, the lead contained in solder on external terminals has presented special problems. Fuji Electric has already begun eliminating lead from its power ICs and power discretes, and has been delivering lead-free products upon request to its customers. Fuji Electric also plans to phase-in the supply of lead-free power module products.

6. Conclusion

Fuji Electric looks forward to continuing its contribution to the advancement of both social development and global environmental protection through innovating and promoting power electronics technology. Power semiconductors are important products that form a pillar of support for such efforts, and this paper has discussed the present status and future outlook for the major products of power semiconductors.

In response to questions of whether social development and global environmental protection can be advanced simultaneously, and whether science and technological development contribute to the well-being of society, although some people may have negative opinions, the answer can only be known by those people who will live in the world 1,000 or 10,000 years from now. Living in the 21st century as individuals whose occupation involves technology and as individuals engaged in the manufacturing industry, we intend to promote technology to advance both social development and global environmental protection, and to develop and commercialize products to contribute to the well-being of society, so that the answer to those questions will be known.

References

(1) Energy Information Administration. U.S. Department of Energy, International Energy Outlook 2004. 2004-04.

(2) Intergovernmental Panel on Climate Change.Summary for Policymakers. Third Assessment Report. 2001-09.

(3) Otsuki, M. et al. Investigation on the Short-Circuit Capability of 1200 V Trench Gate Field Stop IGBTs. Proceedings of ISPSD'02, 2002. p.281-284.

(4) Otsuki, M. et al. 1200 V FS-IGBT Module with Enhanced Dynamic Clamping Capability. Proceedings of ISPSD'04. 2004. p.339-342.

(5) Takei, M. et al. 1200 V Reverse Blocking IGBT with Low Loss for Matrix Converter. Proceedings of ISPSD '04. 2004. p.125-128.

(6) Kamata, I. et al. Influence of 4H-SiC Growth Conditions on Micropipe Dislocation. Japan Journal of Applied Physics. vol.41, part 2, no.10B, 2002, p.L1137-L1139.

(7) Nakamura, D. et al. Ultrahigh-quality silicon carbide single crystals. Nature. vol.430, 2004, p.1009-1012.

(8) Iwamuro, N. et al. A new concept for high voltage MCCT with no J-FET resistance by using a very thin wafer, IEEE IEDM Tech. Dig. 1997, p.351.

(9) Ikeda, N. et al. Study of Lead Free Solder Joint to Power Devices and Thermal Performance. MATE'04. 2004, p.375-378.

(10) Nishimura, Y. et al. New Generation Metal Base Free IGBT Module Structure with Low Thermal Resistance. Proceedings of ISPSD'04. 2004, p.347-350.

(11) Kobayashi, T. et al. High-Voltage Power MOSFET Reached Almost to the Silicon Limit. Proceedings of ISPSD'01. 2001, p.435-438.

(12) Fujihira, T. Theory of Semiconductor Superjunction Devices. Japan Journal of Applied Physics. vol.36, 1997, p.6254-6262.

(13) Onishi, Y. et al. 24 mΩcm^2 680 V Silicon Superjunction MOSFET. Proceedings of ISPSD'02. 2002, p.241-244.

(14) Yamazaki, T. et al. Low Qgd Trench Power MOSFETs with Robust Gate for Automotive Applications. Proceedings of PCIM Europe. Power Electronics, 2003, p.263-268.

(15) Yoshida, K. et al. Surge Protection IC for the Switch Interface of ECUs. Proceedings of 2nd International Conference on Integrated Power Systems. 2002, p.139-145.

(16) Fujishima, N. ; Salama, C. A. T. A Trench Lateral Power MOSFET using Self-Aligned Trench Bottom Contact Holes, Proceedings of IEDM'97, 1997, p.359-362.

(17) Fujishima, N. et al. A 700 V Lateral Power MOSFET with Narrow Gap Double Metal Field Plates Realizing Low On-resistance and Long-term Stability of Performance. Proceedings of ISPSD'01. 2001, p.255-258.

U4-series IGBT Modules

Kouichi Haraguchi
Shuji Miyashita
Yuichi Onozawa

1. Introduction

General-purpose inverters, uninterruptible power supplies (UPSs) and other types of power conversion equipment are subject to never-ending demands for higher efficiency, smaller size, lower cost and lower noise. Moreover, higher performance, lower cost and higher reliability are also required of the power semiconductor devices used in the inverter circuits of such equipment. In recent years, the IGBT (insulated gate bipolar transistor) have become the most prevalent power semiconductor element due to its low loss, easy drive circuit implementation and high ruggedness.

Fuji Electric first developed commercial IGBTs in 1988, and since then has accelerated efforts to improve the characteristics and reliability of those devices. Fuji Electric has also developed a new 5th generation of IGBT modules (U-series)(1) that use IGBTs having trench and field-stop (FS) structures(2).

This paper introduces Fuji Electric's latest device technology and product series, using the example of the U4-series EconoPACK-plus*1 1,200 V breakdown voltage IGBT module developed for the purpose of improving noise suppression and higher performance.

2. Characteristics of the U4-series IGBT Module

2.1 Concept

Fuji Electric has previously developed a trench gate IGBT based on trench-type power MOSFET (metal oxide semiconductor field-effect transistor) technology.

The U4-series realizes further improvements in the performance characteristics based on this technology, and was developed to achieve the following objectives.

(1) Lower loss generated by the device itself

By using a configuration in which the p-layer and emitter of a conventional trench-type IGBT chip are shorted via a high resistance R_s, the newly developed U4-series IGBT module (hereafter referred to as U4-IGBT) aims to improve controllability of the turn-on speed and to realize 30 % lower turn-on loss compared to the conventional trench-type IGBT. U4-IGBT aims almost the similar level of turn-off loss and reverse recovery loss as the conventional type.

(2) Narrow distribution of device characteristics in order to facilitate implementation of parallel connections

By using U4-series FWD (free wheeling diode) (hereafter referred to as the U4-FWD), the U4-series aims to reduce the distribution in forward voltage (V_F) to 0.3 V or less in order to facilitate the implementation of parallel connections, and to realize a high-speed soft recovery characteristic.

(3) Low EMI noise when installed in actual equipment

Although the FWD reverse recovery characteristic is considered to be the main factor that determines the EMI noise during switching, the FWD characteristic is not the only factor. In fact, the characteristics of the IGBT chip determine the reverse recovery characteristic of the FWD chip. The noise level changes according to the matching between the IGBT chip and the FWD chip, and therefore, it was planned to reduce the level of noise by optimizing the characteristics of both the IGBT and FWD chips.

(4) Reuse of conventional technology

The U4-series package is intended to be used in the same manner as a conventional IGBT module, and therefore, redesign of the main circuit, cooling fins and the like was unnecessary.

2.2 U4-IGBT chip features

Figure 1 compares the structures of the U4-IGBT chip and a conventional trench IGBT chip, and Fig. 2 shows the relationship between IGBT capacitance and the turn-on characteristic. By shorting the p-layer and emitter with the high-resistance R_s, a Miller capacitance (C_{res}) actually smaller than that of a conventional IGBT can be realized.

In a conventional trench IGBT, the gate is fabricated in a trench configuration, and since there is no JFET (junction field effect transistor) component corresponding to a planar IGBT, the collector-emitter

---

[1] EconoPACK-plus is a trade mark of Eupec GmbH. Warstein.

saturation voltage ($V_{CE(sat)}$) decreases but capacitance increases due to the trench configuration. In particular, if C_{res} is large, the turn-on switching-speed becomes slower and switching loss increases. Therefore, in order to reduce the switching loss at turn-on, it is effective to make C_{res} smaller and to optimize the ratio between input capacitance (C_{ies}) and C_{res}. In the development of the U4-IGBT, simulations and verification testing were performed to optimize these issues.

Figure 3 compares the turn-on switching waveforms of the conventional trench IGBT and the U4-IGBT. Since the effective C_{res} has been reduced due to the R_s shown in Fig. 1, the collector-emitter voltage (V_{CE}) tail is short, and as a result, the turn-on loss is less than that of a conventional trench IGBT. Moreover, even if the gate resistance (R_G) is increased, since the tail voltage is small, the turn-on loss will be relatively low, thereby expanding the range over which the turn-on speed can be controlled by R_G.

Figure 4 shows the I_C–V_{CE} characteristic of the U4-IGBT.

Since a positive temperature coefficient can be obtained as in a conventional trench IGBT, the current unbalance during a parallel connection is mitigated, and parallel connections to a large capacity inverter circuit or the like are easy to implement.

2.3 U4-FWD features

Recent general-purpose inverters tend to increase torque during low-frequency output, and the thermal duty of the FWD is large. Moreover, as with the IGBT, it is important to equalize the current balance when the FWD is in a parallel connection. For this purpose, a new diode having less distribution in its V_F characteristic is needed. Since the newly developed U4-FWD aims for higher reliability, it uses an FZ (floating zone) wafer that is not a significant cause of such distribution. The result is V_F variation of 0.3 V or less, which is comparable to that of the IGBT, thereby eliminating

Fig.1 Comparison of conventional trench IGBT and U4-IGBT chip structures

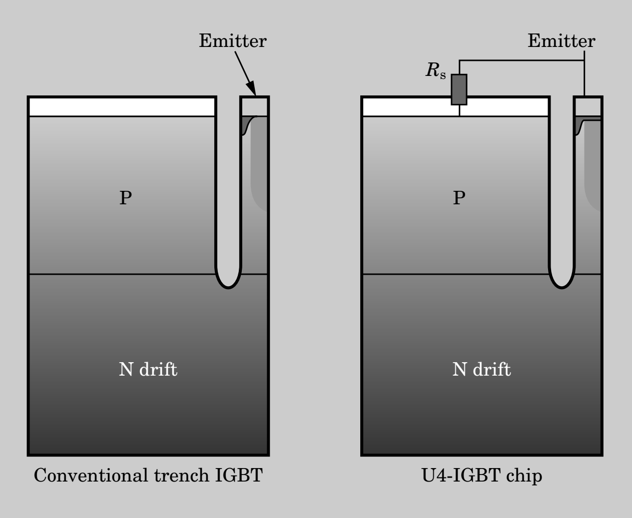

Fig.2 Relation between IGBT capacitance and turn-on characteristic

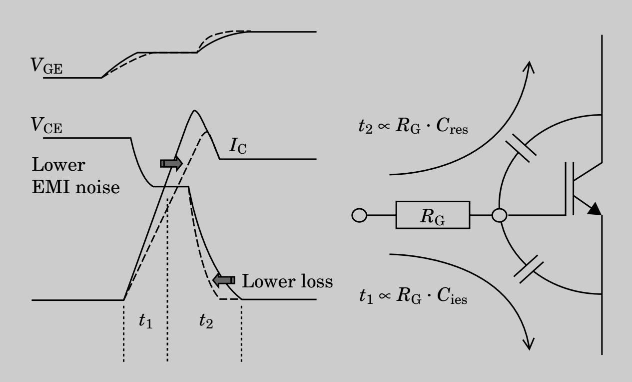

Fig.3 Comparison of conventional trench IGBT and U4-IGBT turn-on waveforms

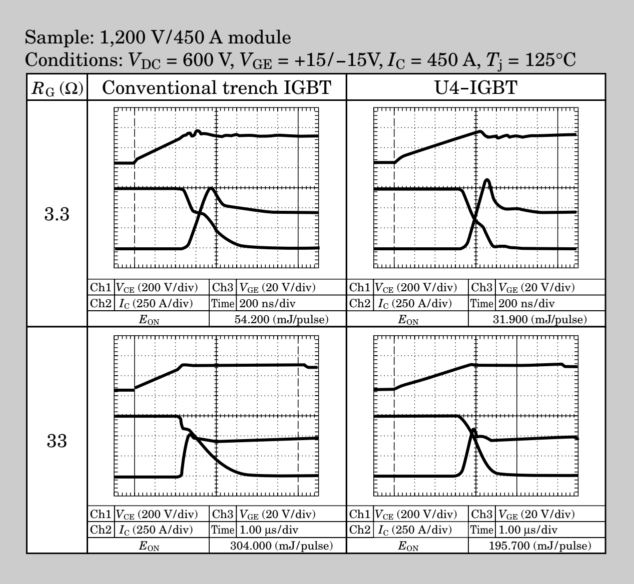
Sample: 1,200 V/450 A module
Conditions: V_{DC} = 600 V, V_{GE} = +15/−15V, I_C = 450 A, T_j = 125°C

R_G (Ω)	Conventional trench IGBT	U4-IGBT
3.3	Ch1 V_{CE} (200 V/div), Ch3 V_{GE} (20 V/div) Ch2 I_C (250 A/div), Time 200 ns/div E_{ON} 54.200 (mJ/pulse)	Ch1 V_{CE} (200 V/div), Ch3 V_{GE} (20 V/div) Ch2 I_C (250 A/div), Time 200 ns/div E_{ON} 31.900 (mJ/pulse)
33	Ch1 V_{CE} (200 V/div), Ch3 V_{GE} (20 V/div) Ch2 I_C (250 A/div), Time 1.00 µs/div E_{ON} 304.000 (mJ/pulse)	Ch1 V_{CE} (200 V/div), Ch3 V_{GE} (20 V/div) Ch2 I_C (250 A/div), Time 1.00 µs/div E_{ON} 195.700 (mJ/pulse)

Fig.4 I_C–V_{CE} characteristic of U4-IGBT

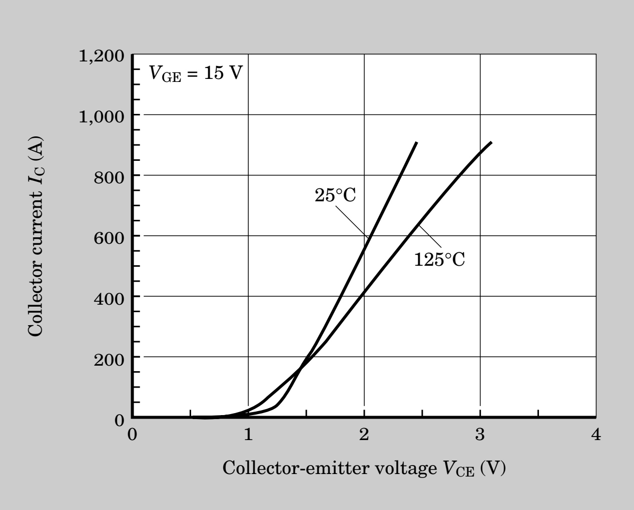

the need for V_F classification for parallel connection module implementations, and facilitating the implementation of parallel connections of modules for large-capacity inverters.

Figure 5 compares the structures of the conventional FWD and the U4-FWD. For the use of an FZ wafer, it is necessary to optimize the crystal profile of the FZ wafer in order to reduce surge voltage during reverse recovery and to achieve a low V_F. We simulated the carrier profile and reverse recovery characteristic to derive the optimal values.

Figure 6 shows the simulated results and actual measured waveforms of the low-current reverse recovery characteristic. As a result, the combination of the U4-IGBT and U4-FWD inhibits the generation of oscillation and surge voltage due to low-current reverse recovery, and contributes to the streamlining of the snubber circuit and reduction of EMI noise.

Figure 7 shows the I_F–V_F characteristic of the U4-FWD. Since a positive temperature coefficient can be obtained as with the U4-IGBT, the U4-FWD is effective in balancing the current during a parallel implementation.

2.4 Comparison of EMI noise

When an IGBT module is installed in actual equipment, EMI noise is generated and radiates out to the exterior, and the level of that noise is regulated by

Fig.5 Comparison of conventional FWD and U4-FWD structures

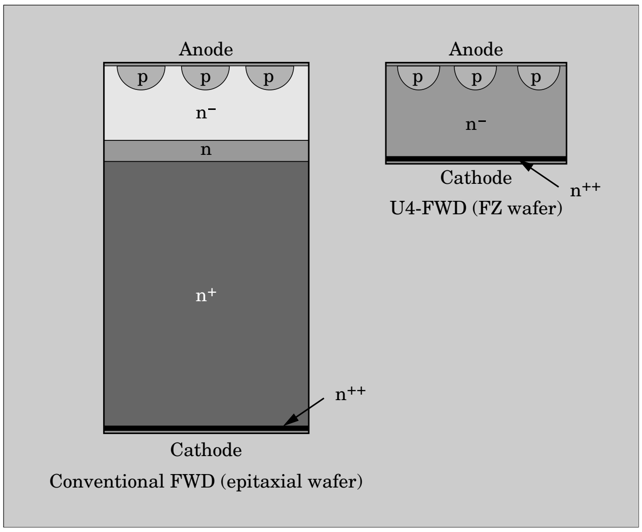

Fig.6 Simulated and measured waveforms of low-current reverse recovery characteristic

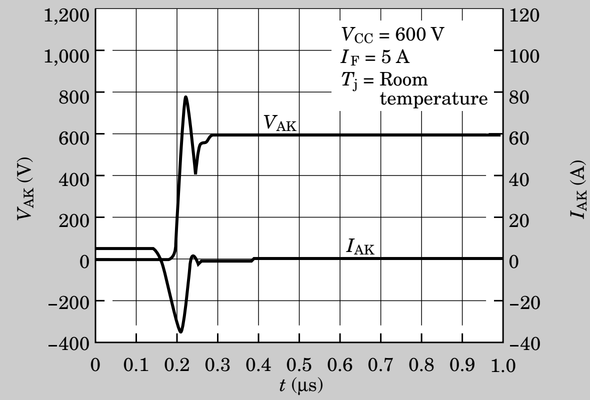

U4-FWD low-current reverse recovery
Simulation

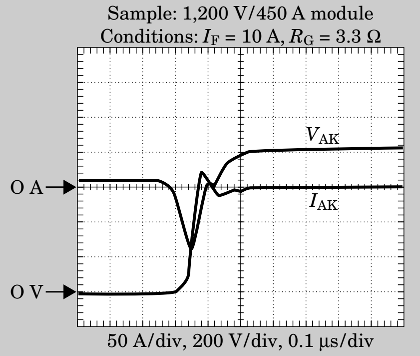

U4-FWD low-current reverse recovery measured waveform
(U4-IGBT + U4-FWD)

Fig.7 I_F–V_F characteristic of U4-FWD

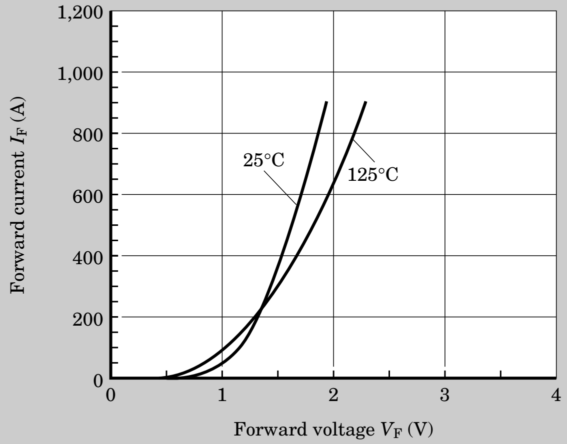

Fig.8 EMI noise-generating mechanism and simplified measurement method

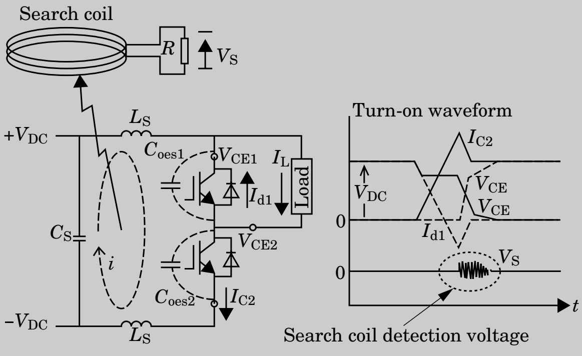

the European standard EN61800-3 and the like. Figure 8 shows the EMI noise-generating mechanism and a method for measuring that noise. With this method, noise measurement is easy to implement. It has been reported that oscillation due to the resonance circuit between the IGBT module and snubber circuit is the source of the EMI noise. That oscillation is triggered by the values of *di*/*dt* and *dv*/*dt* during switching. The *di*/*dt* and *dv*/*dt* are determined by the IGBT turn-on characteristic, and the FWD reverse recovery characteristic is similarly determined by the turn-on characteristic. Thus, to reduce EMI noise, it is necessary to optimize both the FWD and IGBT characteristics.

Figure 9 compares the EMI noise (3 m method) during a DC chopper test. The U4-IGBT achieved improved R_G controllability of the turn-on speed and less turn-on switching loss, the U4-IGBT generates less EMI noise than a conventional trench IGBT and also dissipates less device power loss under the same gate drive conditions.

Fig.9 Comparison of EMI noise during DC chopper test

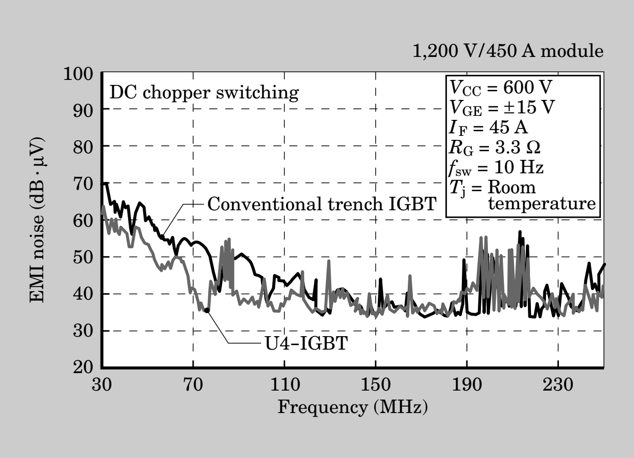

3. U4-IGBT Product Lineup

Fuji Electric has combined the abovementioned U4-IGBT technology and U4-FWD technology, while continuing to utilize the package technology of high-power cycling capable U-IGBT modules, to complete the development and establish a product line of U4-IGBT EconoPACK-plus modules, which provide improved performance compared to the conventional trench IGBT modules.

Figure 10 shows examples of U4-IGBT packages

Fig.10 Examples of U4-IGBT packages

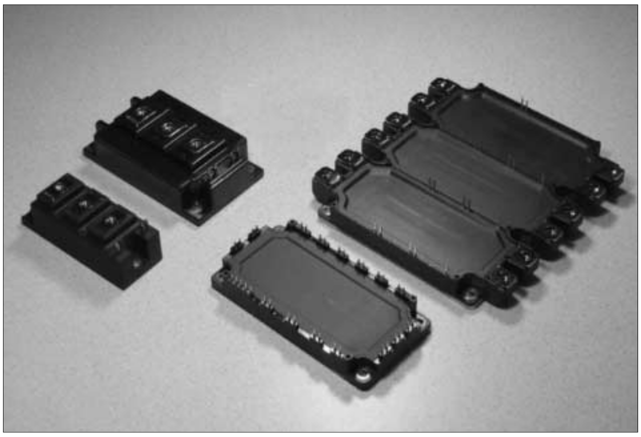

Table 1 U4-IGBT product lineup

Voltage rating	Package	I_C rating												
		50 A (11 kW)	75 A	100 A (22 kW)	150 A	225 A 200 A (40 kW)	300 A	450 A 400 A (75 kW)	600 A	800 A	1,200 A	1,600 A	2,400 A	3,600 A
1,200 V	PIM		EP3											
	6 in 1	New PC2 with NTC												
			New PC3 with NTC											
						EconoPACK-plus (6 in 1)								
	2 in 1				M232	M233								
						M235								
						M249			M248					
	1 in 1							M127		M138	M142		M143	
1,700 V	6 in 1			New PC3 with NTC		EconoPACK-plus (6 in 1)								
	2 in 1					M249			M248					
	1 in 1										M142		M143	

and Table 1 lists details of the IGBT module package product lineup.

The new U4-IGBT modules are available in a variety of packages in two product lines having breakdown voltages of 1,200 V and 1,700 V, respectively, and having current ratings ranging from 50 to 3,600 A. This wide range of products can be applied to various types of power conversion equipment.

4. Conclusion

The U4-IGBT and U4-FWD technologies, characteristics, and product lineup of IGBT modules has been presented above. These products make full use of the latest semiconductor technology and package technology to realize lower loss devices, and we are confident that these products will make significant contributions toward achieving smaller size and lower loss in equipment having inverter circuits.

Fuji Electric is committed to the future development of devices having even higher performance and reliability, and intends to enhance its own technology while contributing to the development of power electronics.

References

(1) Laska, T. et al. The Field Stop IGBT (FS IGBT) A New Power Device Concept with a Great Improvement Potential. Proc. 12th ISPSD. 2000, p.355-358.

(2) Otsuki, M. et al. 1200 V FS-IGBT module with enhanced dynamic clamping capability. Proc. ISPSD'04. 2004, p.339-342.

High-power IGBT Modules for Industrial Use

Takashi Nishimura
Hideaki Kakiki
Takatoshi Kobayashi

1. Introduction

Power devices used in industrial-use high capacity inverter system applications are predominately GTO (gate turnoff) thyristors, which easily handle high voltages and currents. However, recent advances in high-voltage and high-power technology for IGBT (insulated gate bipolar transistor) modules have been remarkable, and IGBT modules are being used nowadays in applications that had previously required the use of GTO thyristors. IGBT modules have an insulated module structure that differs from the pressure contact structure of a GTO thyristor and that facilitates assembly, use and maintenance, and as a result, the field of IGBT module applications is expanding exponentially.

In response to the diversifying needs of recent years, Fuji Electric has been actively developing products for the recently growing market of high-power applications.

Targeting high-power industrial-use applications, Fuji Electric has equipped its U4-series of chips (hereafter referred to as U4-chips), an improved version of its U-series of chips (hereafter referred to as U-chips), with a copper base to develop high-power IGBT modules having current capacities of 1,600 A for a 130 × 140 (mm) (1-in-1 and 2-in-1) package and 3,600 A for a 190 × 140 (mm) (1-in-1) package, and high-voltage ratings of 1,200 V and 1,700 V. This paper introduces the summary and technical development of the modules.

2. Product Lineup

Table 1 shows Fuji Electric's product lineup of high-power IGBT modules. The module lineup consists of 1,200 V and 1,700 V voltage classes, three types of packages, and current ratings of 600 to 3,600 A among a total of 14 types of products. Figure 1 shows an external view of the packages.

3. Electrical Characteristics

Electrical characteristics of modules that use U4-chips are described below in comparison to modules that use U-chips, and the 2MBI1200U4G-170 (2-in-1 1,200 A/1,700 V) is presented at the representative model.

Table 1 Fuji Electric's product lineup of high-power IGBT modules

	Model number	Rated voltage (V)	Rated current (A)	Package size (mm)	Package type
1 in 1	1MBI1200U4C-120	1,200	1,200	130 × 140 × 38	M142
	1MBI1600U4C-120		1,600		
	1MBI2400U4D-120		2,400	190 × 140 × 38	M143
	1MBI3600U4D-120		3,600		
	1MBI1200U4C-170	1,700	1,200	130 × 140 × 38	M142
	1MBI1600U4C-170		1,600		
	1MBI2400U4D-170		2,400	190 × 140 × 38	M143
	1MBI3600U4D-170		3,600		
2 in 1	2MBI600U4G-120	1,200	600	130 × 140 × 38	M248
	2MBI800U4G-120		800		
	2MBI1200U4G-120		1,200		
	2MBI600U4G-170	1,700	600		
	2MBI800U4G-170		800		
	2MBI1200U4G-170		1,200		

Fig.1 External view of Fuji Electric's high-power IGBT modules

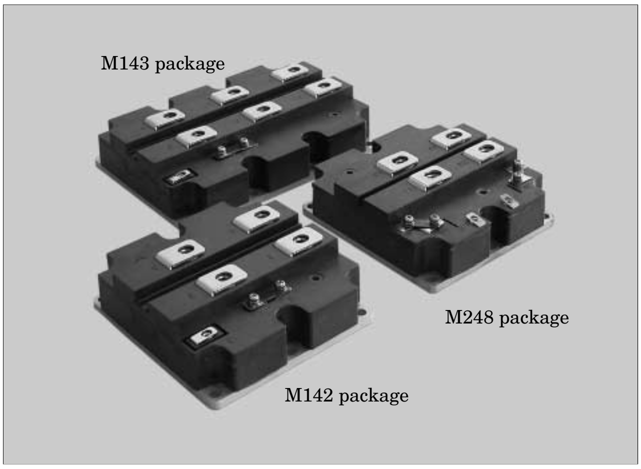

3.1 Absolute maximum ratings and electrical characteristics

Table 2 lists the absolute maximum ratings and electrical characteristics.

Table 2 Maximum ratings and electrical characteristics (model No.: 2MBI1200U4G-170)

(a) Maximum ratings (T_j = T_c = 25°C, unless otherwise specified)

Item	Symbol	Condition		Maximum rating	Unit
Collector – emitter voltage	V_{CES}	V_{GE} = 0 V		1,700	V
Gate – emitter voltage	V_{GES}	–		±20	V
Collector current	$I_{C(DC)}$	Continuous	T_c = 80°C	1,200	A
	$I_{C(pulse)}$	1 ms	T_c = 80°C	2,400	A
Max. power dissipation	P_C	1 device		4,960	W
Max. junction temperature	$T_{j\ max}$	–		150	°C
Storage temperature	T_{stg}	–		−40 to +125	°C
Isolation voltage	V_{iso}	AC : 1 ms		3,400	V

(b) Electrical characteristics (T_j = T_c = 25°C, unless otherwise specified)

Item	Symbol	Test condition		Min.	Typ.	Max.	Unit
Zero gate voltage collector current	I_{CES}	V_{GE} = 0 V T_j = 125°C V_{CE} = 1,700 V		–	–	1.0	mA
Gate – emitter leakage current	I_{GES}	V_{GE} = ±20 V		–	–	1.6	µA
Gate – emitter threshold voltage	$V_{GE(th)}$	V_{CE} = 20 V I_C = 1.2 A		5.5	6.5	7.5	V
Collector – emitter saturation voltage (sence terminal)	$V_{CE(sat)}$	V_{GE} = +15 V I_C = 1,200 A	T_j = 25°C	–	2.25	–	V
			T_j = 125°C	–	2.65	–	
Input capacitance	C_{ies}	V_{GE} = 0 V V_{CE} = 10 V f = 1 MHz		–	110	–	nF
Turn-on time	t_{on}	V_{CC} = 900 V I_C = 1,200 A V_{GE} = ±15 V R_G = +4.7/− 1.2 Ω T_j = 125°C		–	3.10	–	µs
	t_r			–	1.25	–	
Turn-off time	t_{off}			–	1.45	–	
	t_f			–	0.25	–	
Forward on-voltage (sence terminal)	V_F	V_{GE} = 0 V I_F = 1,200 A	T_j = 25°C	–	1.80	–	V
			T_j = 125°C	–	2.00	–	
Reverse recovery time	t_{rr}	V_{CC} = 900 V I_F = 1,200 A T_j = 125°C		–	0.45	–	µs

(c) Thermal characteristics

Item	Symbol	Condition	Min.	Typ.	Max.	Unit
Thermal resistance (for 1 device)	$R_{th(j-c)}$	IGBT	–	–	0.0252	K/W
		FWD	–	–	0.042	

3.2 *V-I* characteristics

Figure 2 shows the $V_{CE(sat)}$−I_C characteristics and Fig. 3 shows the V_F−I_F characteristics. The saturation voltage of the IGBT chip was designed to decrease the injection efficiency of the pnp transistor, and without applying lifetime control, to increase the transport efficiency and provide a positive temperature coefficient. Moreover, by optimizing lifetime control of the FWD (free wheeling diode) chip, the forward on-voltage is provided with a positive temperature coefficient as in the IGBT, and this is advantageous for parallel connections to both the IGBT chip and the FWD chip.

3.3 Switching characteristics

(1) Turn-on characteristic

Modules that use the U4-chip employ a new structure in order to optimize the balance between input capacitance (C_{ies}) and reverse transfer capacitance (C_{res}), and as a result, their turn-on loss is drastically reduced. Figure 4 shows turn-on waveforms for an inductive load under the conditions of V_{CC} = 900 V, I_C = 1,200 A, R_{gon} = 1.8 Ω and T_j = 125°C. When driven with the same gate resistance (R_{gon}), the module that used the U4-chip (U4-module) had a smaller tail voltage and approximately 50 % less turn-on loss (E_{on}) than the module that used the U-chip (U-

Fig.2 $V_{CE(sat)}$− I_C characteristics

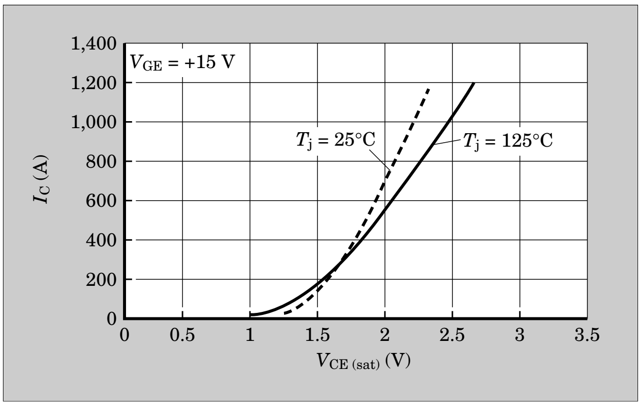

Fig.3 V_F− I_F characteristics

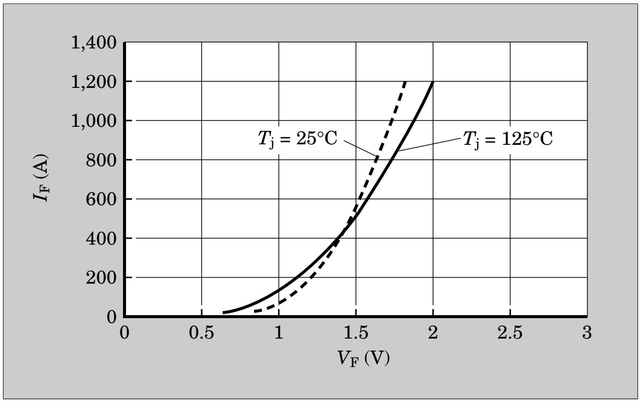

Fig.4 Turn-on waveforms (V_{CC} = 900 V, I_C = 1,200 A, 125°C)

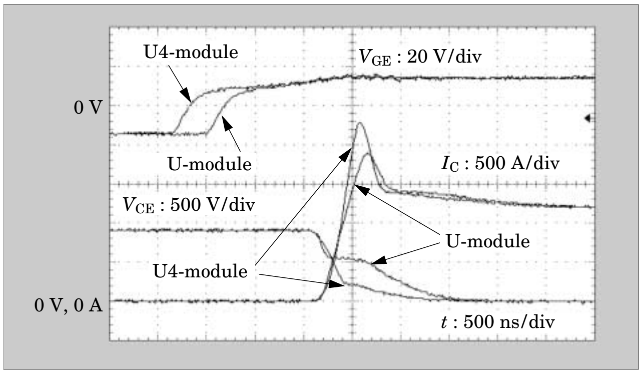

Fig.5 Turn-off waveforms (V_{CC} = 900 V, I_C = 1,200 A, 125°C)

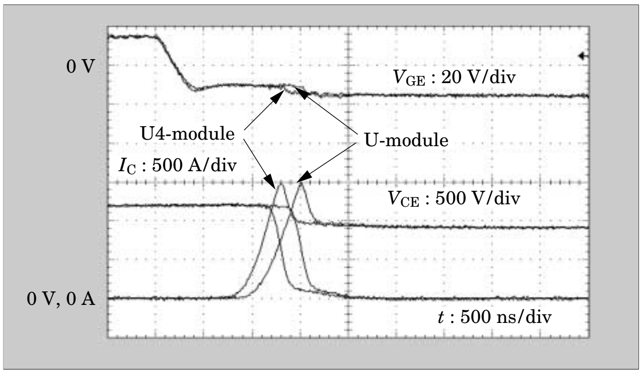

Fig.6 PWM inverter power loss simulation

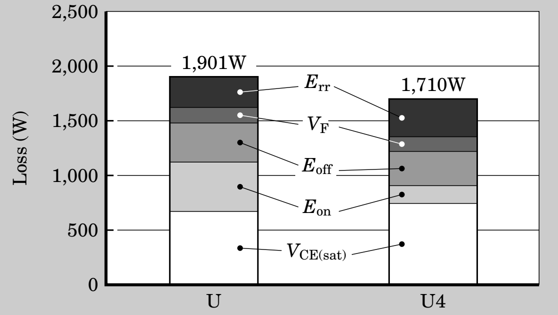

(a) Generation mode (cosϕ = 0.9)

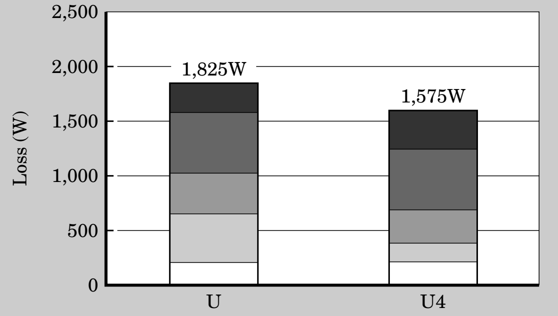

(b) Regeneration mode (cosϕ = – 0.9)

Fig.7 Low-current reverse recovery characteristics

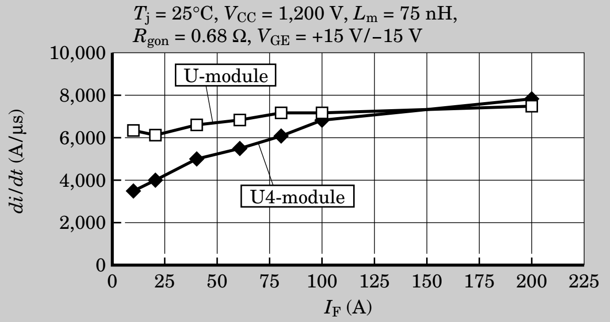

(a) $di/dt - I_F$

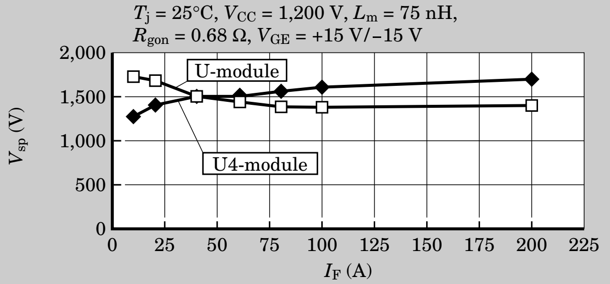

(b) $V_{sp} - I_F$

Fig.8 Low-current reverse recovery waveforms (V_{AK} = 1,200 V, I_F = 10 A, 25°C)

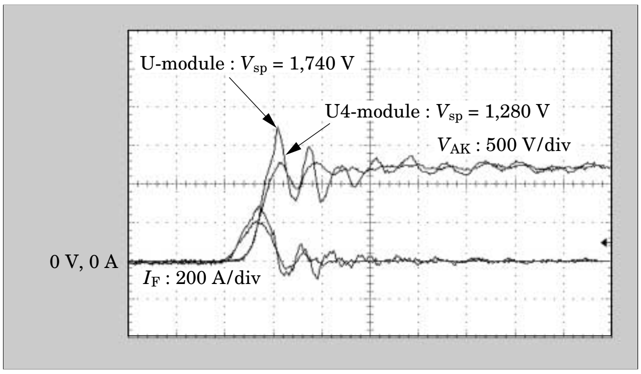

module).

(2) Turn-off characteristic

Figure 5 shows turn-off waveforms for an inductive load under the conditions of V_{CC} = 900 V, I_C = 1,200 A, R_{goff} = 1.2 Ω and T_j = 125°C. When driven with the same gate resistance (R_{goff}), the turn-off loss was approximately 5 % lower for the U4-module than for the U-module.

(3) PWM inverter power loss simulation

Figure 6 shows the results of a simulation of inverter power loss when operated under the same conditions (I_{out} = 860 A_{rms}, cosϕ = 0.9 and – 0.9, f_c = 2.5 kHz). The power loss generated in the U4-module was approximately 10 % less during generation mode and approximately 14 % less during regeneration mode than that of the U-module.

(4) Low-current reverse recovery characteristics

The characteristic features of U4-modules, reduced low-current turn-on di/dt and improved gate resistance controllability of the turn-on di/dt, enable suppression of the surge voltage at the event of reverse recovery. Figure 7 shows the low-current reverse recovery characteristics. It can be seen that the low-current turn-on *di*/*dt* is smaller and that surge voltage is suppressed to a greater extent for the U4-module in comparison to the U-module. Figure 8 shows waveforms obtained under the conditions of V_{AK} = 1,200 V, I_F = 10 A, and R_{gon} = 0.68 Ω. From this figure and from Fig. 7(b), it can be seen that the surge voltage is decreased from 1,740 V to 1,280 V.

4. Package Technology for High-power IGBT Modules

High capacity inverter systems require high reliability, and ensuring the reliability of the power devices used to construct such systems is extremely important. To realize power devices with greater capacity, it is necessary that many chips be connected in parallel inside a module, and it is important that the current balance and generation of heat are maintained with an equal distribution.

4.1 Chip characteristics

As described in paragraph 3.2, high-power IGBT modules are equipped with chips having a positive temperature coefficient. In chips having a positive temperature coefficient, a rise in the junction temperature causes voltage to increase, and therefore current is self-regulated in order to equalize the junction temperature in chips connected in parallel. This characteristic is used to configure stably operating modules.

4.2 Divided DCB substrate

High-power IGBT modules are configured with a maximum of twenty-four IGBT and FWD chips, each, which are connected in a parallel configuration. In order to ensure power cycle capability and to improve mass productivity, a structure is adopted that divides the DCB (direct copper bonding) substrate. By dividing the DCB substrate, thermal interference can be reduced and the quality of each DCB substrate can be checked individually, and as a result, productivity can be increased. Figure 9 shows the internal structure of a high-power IGBT module.

Fig.9 Internal structure

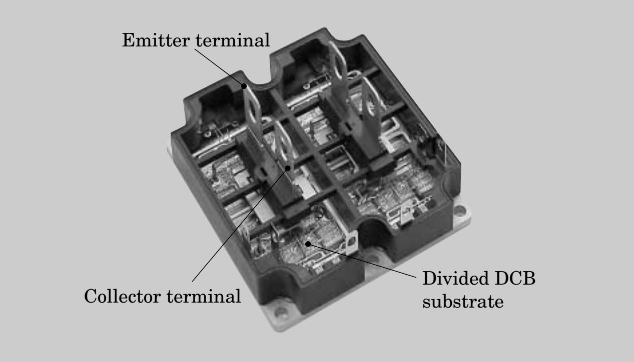

4.3 Optimization of main terminal structure

The following three factors are important in the design of the main terminal structure.

(1) Equalization of current balance among DCB substrates
(2) Reduction of internal inductance
(3) Suppression of temperature rise due to heat generated at main terminal

These three factors involve complex mutually interacting tradeoff relations, and an optimized design that satisfies the requirements of all three of these factors is indispensable.

(1) Equalization of current balance

The DCB substrate is divided from the location of the module's main terminal into a portion located directly below the emitter terminal and a portion located directly below the collector terminal, and these must be connected in parallel with the shortest wiring possible. However, the implementation of the shortest possible wiring results in a structure prone to inductance imbalance between DCB substrates, and a large current imbalance will occur during switching (turn-on, turn-off, and reverse recovery). Figure 10 shows the difference of currents flowing to the DCB substrate in the case of an inductance imbalance and in the case of balanced inductance. To balance the inductance,

Fig.10 Measurement of current between DCB substrates

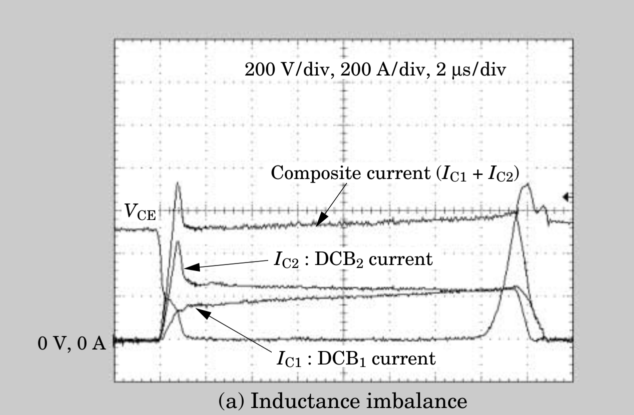

(a) Inductance imbalance

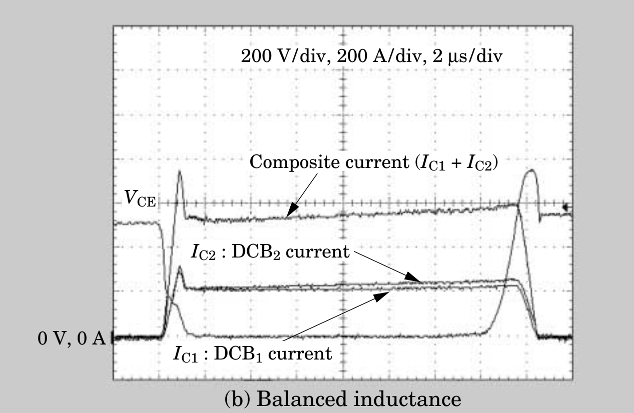

(b) Balanced inductance

Fig.11 ΔT_j power cycle capability

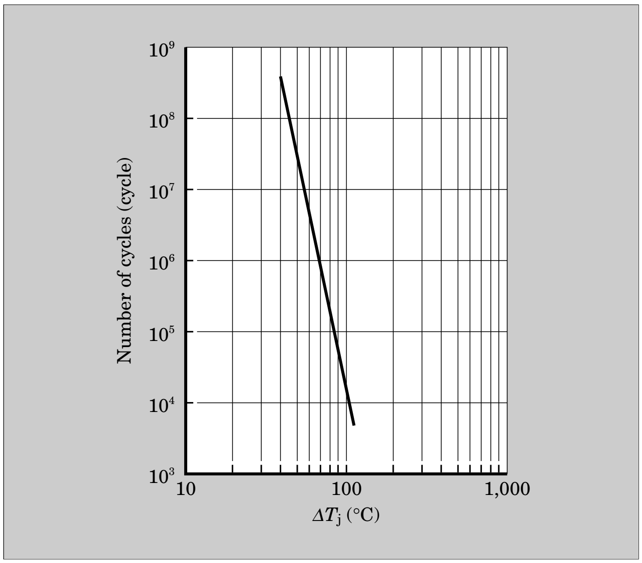

current pathways inside the emitter terminal and collector terminal were analyzed, and a structure was adopted that balances the current.

(2) Reduction of internal inductance

High-power IGBT modules require the capability to instantaneously turn-off a large current, and it is important to reduce the surge voltage generated inside the package at the event of turn-off. In other words, decreasing the internal inductance of the package becomes an issue. However, the structure described in the above paragraph and introduced to equalize the current balance has the contrary effect of increasing the internal inductance, but by actively utilizing magnetic field interactions, individual inductances can be cancelled and the increase in inductance suppressed. As a result, an extremely small inductance per terminal of approximately 20 nH was realized.

(3) Suppression of temperature rise due to heat generated at main terminal

The main terminal of a high-power IGBT module is required to provide the capability to conduct 1,200 A of current per terminal (single terminal configured from the emitter and collector terminals) in order to configure a 3,600 A (max.) module. The extent to which temperature rise due to the heat generated by a terminal during current conduction can be suppressed is an issue. By forming the emitter and collector terminals with an outward curvature at their part inside module, the volume of each terminal increases and the temperature rise due to generated heat during current conduction is suppressed.

5. Ensuring the Power Cycle Capability

From the analysis of an IGBT module after power cycle testing, Fuji Electric has verified that the ΔT_j power cycle capability is determined by the combined lifetimes of the under-the-chip solder and the bonding wire. In a high-power IGBT module, by using the higher stiffness material of Sn-Ag as the under-the-chip solder, dividing the DCB substrate to suppress thermal interference, and equalizing current flow among DCB substrates, we verified that the ΔT_j power cycle capability is equal to that of a module having few parallel connections (See Fig. 11). Moreover, we conducted a ΔT_c power cycle test assuming a specific application for high-power IGBT modules in which the case temperature varied widely, and verified the capability to withstand 10,000 cycles at $\Delta T_c = 70°C$.

6. Conclusion

An overview of Fuji Electric's high-power IGBT module products that use U4-chips has been presented. We are confident that this product group will be able to provide through support of diversified needs. In particular, the reduction in turn-on loss enables a wider range of choices for the gate resistance and improves the ease of use. Fuji Electric remains committed to raising the level of power semiconductor and package technology in order to support additional needs and to developing new products that contribute to the advancement of power electronics.

Reference

(1) Morozumi, A. et al. Reliability of Power Cycling for IGBT Power Semiconductor Module. Conf. Rec. IEEE Ind. Appl. Conf. 36th. 2001, p.1912-1918.

Lead-free IGBT Modules

Yoshitaka Nishimura
Kazunaga Onishi
Eiji Mochizuki

1. Introduction

In response to environmental issues, lead-free solder (in compliance with the RoHS*[1] directive) is being promoted for use instead of conventional Sn-Pb solder in the mounting of electronic components. Under these circumstances, there is also desire for IGBT (insulated gate bipolar transistor) modules to be made lead-free.

Fuji Electric has been using lead-free solder in the soldered connections underneath silicon chips since 1998, and has succeeded in improving power cycle reliability. This paper reports a new established technique for using lead-free solder instead of Sn-Pb solder for joining a ceramic insulated substrate to a metal base in an IGBT module.

2. Challenges to Achieving Lead-free Status

Figure 1 shows a schematic diagram of the IGBT module, and lists the coefficients of thermal expansion for several component materials. Generally, in an IGBT module, a metal base and ceramic substrate having significantly different coefficients of thermal expansion are joined by soldering. During the soldering process and due to changes in the ambient temperature, the metal base deforms and stress is generated in the area of the soldered joint. This stress causes cracks in the soldered joint. As a result, with lead-free solder, it is difficult to ensure sufficient reliability during thermal cycle testing.

Fig.1 Conventional IGBT module structure

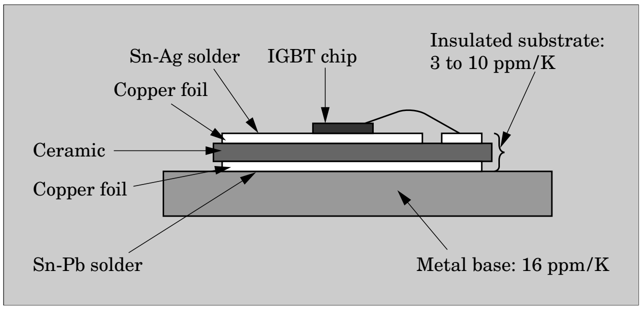

Fig.2 Relationship between ambient temperature and deformation of the metal base

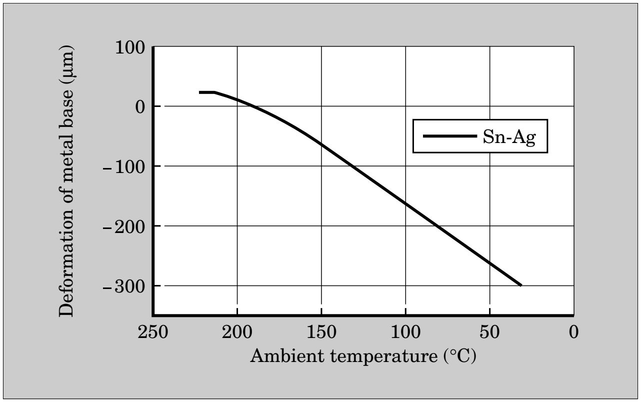

Table 1 Characteristics of various ceramics and copper

Type of material		Coefficient of thermal expansion	Thermal conductivity
Ceramics	Alumina	7 ppm/K	20 W/(m·K)
	Aluminum nitride	4 ppm/K	170 W/(m·K)
	Silicon nitride	3 ppm/K	70 W/(m·K)
Metal base	Copper	16 ppm/K	390 W/(m·K)

Figure 2 shows the relationship between ambient temperature and deformation of the metal base. From this figure it can be understood that deformation of the metal base is caused only by the difference in thermal expansion coefficients of the insulated substrate and metal base. In other words, by reducing the amount of metal base deformation after soldering, the ability to withstand thermal cycle testing can be increased.

3. Considerations in the Structural Design

The structural design was evaluated in order to suppress the amount of metal base deformation due to the difference in thermal expansion coefficients.

Table 1 lists characteristics of various ceramics used in a typical insulated substrate and of the copper in the metal base. Alumina substrates, which are

---

*1: RoHS is Restriction of the use of certain hazardous substances in electrical and electronic equipment.

inexpensive and durable, and aluminum nitride substrates, which are characterized by good thermal conductance, are used as the insulated substrates in IGBT modules.

The use of alumina, which has a coefficient of thermal expansion that is close to that of the metal base, is thought to be effective in increasing the ability of a lead-free IGBT module to withstand thermal cycle testing.

4. Experimental Results

4.1 Alumina ceramic substrate

Figure 3 shows the amount of deformation of the metal base after soldering to various insulated substrates.

(1) By changing from an aluminum nitride to alumina substrate, the amount of deformation after soldering was reduced from 640 μm to 460 μm.

(2) By changing the thickness of the alumina ceramic from 0.635 mm to 0.25 mm, the amount of deformation after soldering was reduced from 460 μm to 330 μm.

When made thinner, the ceramic substrate deforms more easily due to stress. Consequently, the amount of metal base deformation decreases as a result of the ceramic substrate deformation due to stress generated by the difference in thermal expansion coefficients.

Fig.3 Relationship between various insulated substrates and deformation of the metal base

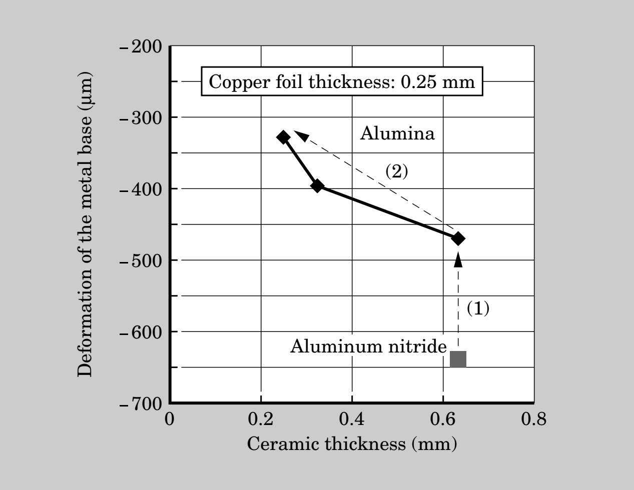

Fig.4 Relationship between the number of thermal cycles tested and solder crack length

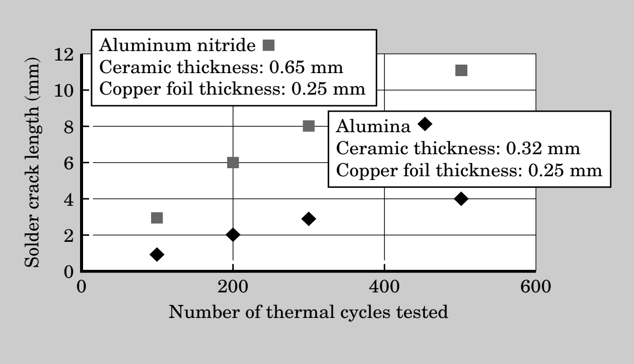

Stress is generated due to a difference in thermal expansion coefficients of the insulated substrate and metal base, and to investigate this phenomenon, we conducted thermal cycle tests using various ceramic substrates.

Figure 4 shows the relationship between the number of thermal cycles tested and the solder crack length. Compared to an aluminum nitride insulated substrate, an alumina substrate results in less deformation of the metal base, fewer solder cracks, and greater ability to withstand thermal cycle testing.

4.2 Consideration of the solder material

Figure 5 shows the relationship between the solidus temperature of various types of solder and the amount of deformation of the metal base. It can be seen that the solidus temperature and metal base deformation have a proportional relationship. To reduce the amount of metal base deformation it is effective to select solder that has a low melting point. For this purpose, we selected and examined low-melting point Sn-Ag solder and Sn-Ag-In solder.

Fig.5 Relationship between the melting point of solder and deformation of the metal base

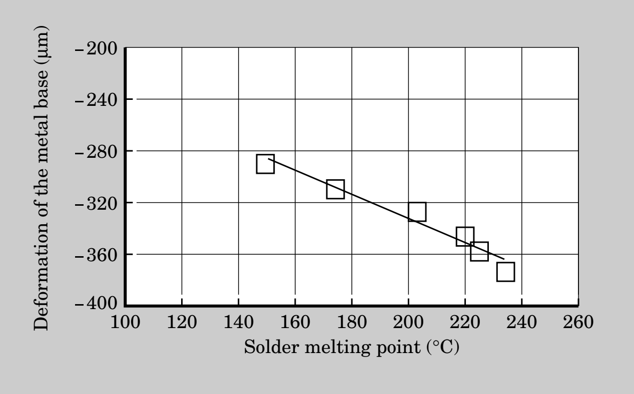

Fig.6 Stress-strain curve for Sn-Ag solder and Sn-Ag-In solder at room temperature

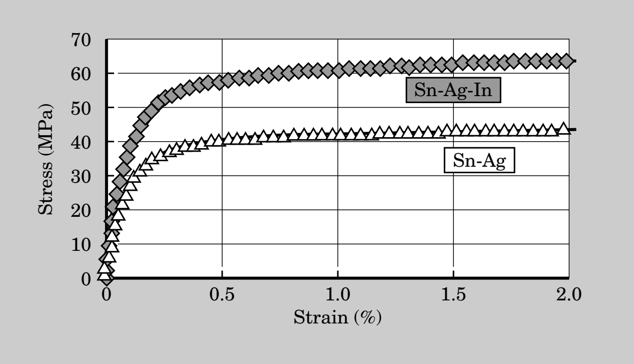

Figure 6 shows the stress-strain curve for Sn-Ag solder and Sn-Ag-In solder at room temperature. The strength of Sn-Ag-In solder has been increased to approximately 1.5 times that of Sn-Ag solder, and the strengths of these materials exhibit similar tendencies even at 125°C. To investigate the effect of solder type on the ability to withstand thermal cycling, we conducted thermal cycling tests (using an alumina ceramic thickness of 0.32 mm and a copper foil thickness of 0.25 mm) in products that currently use alumina substrates.

Fig.7 Ultrasonic monitoring of thermal cycling test results

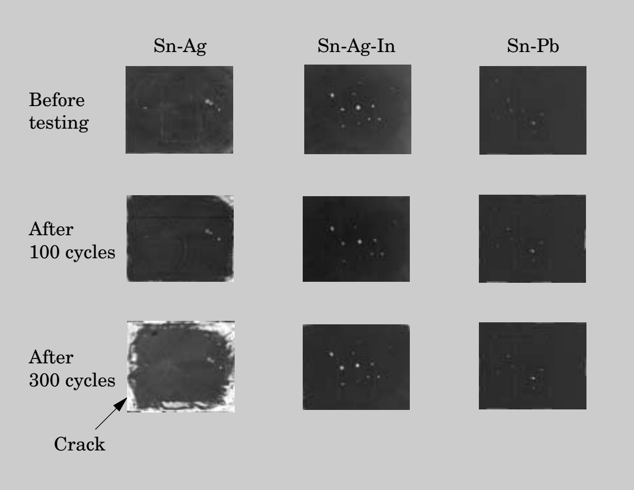

Fig.8 Relationship between the number of thermal cycles tested and solder crack length

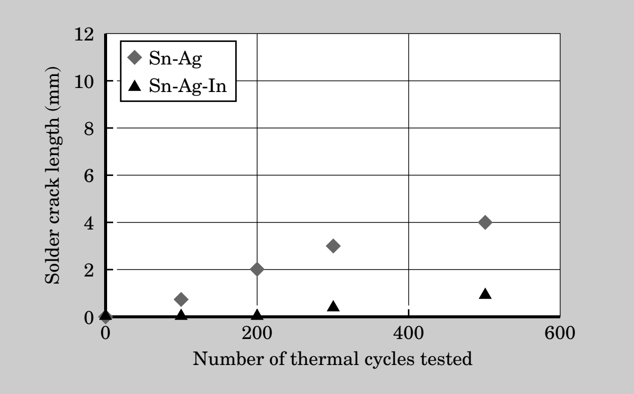

Fig.9 Relationship between solder thickness and crack length

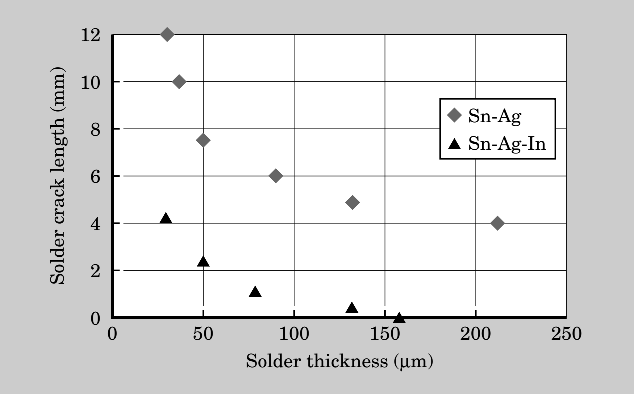

Figures 7 and 8 show the results of ultrasonic inspection of the solder joints. When Sn-Ag solder was used, cracks occurred over approximately 30 % of the solder joint area after a test of 300 thermal cycles, but with the newly developed Sn-Ag-In solder, there were almost no cracks and reliability was nearly the same as that of conventional leaded solder.

Figure 9 shows the relationship between solder thickness and crack length. It can be seen that the effect of solder thickness is less for Sn-Ag-In than for Sn-Ag.

Figure 10 shows the microstructure of the solder, before and after the thermal cycle testing. As a result of the thermal cycle testing, the Sn-Ag solder exhibits grains aggregate. However, the microstructure of Sn-Ag-In solder does not change. Strength generally decreases due to an increase in the grain size. The addition of Indium to Sn-Ag prevents an increase in the grain size and is thought to be one reason for the improvement in ability to withstand thermal cycle testing.

5. IGBT Module that Uses Sn-Ag-In Solder

Figure 11 shows Fuji Electric's RoHS-compliant lead-free IGBT module. Although this product does not use lead or hexavalent chromium, it achieves the same level of product reliability as that of a module

Fig.10 Microstructure of solder

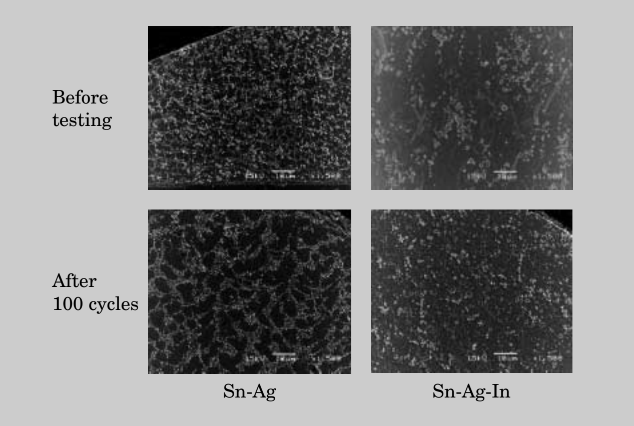

Fig.11 Fuji Electric's RoHS-compliant, lead-free IGBT module

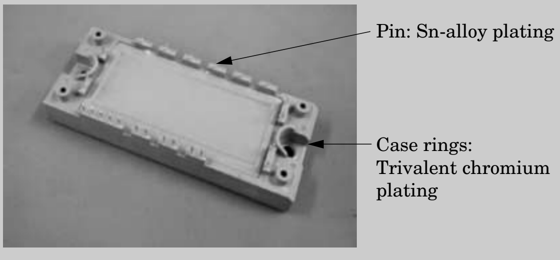

Fig.12 Relationship between copper foil thickness and thermal expansion coefficient of insulation substrate

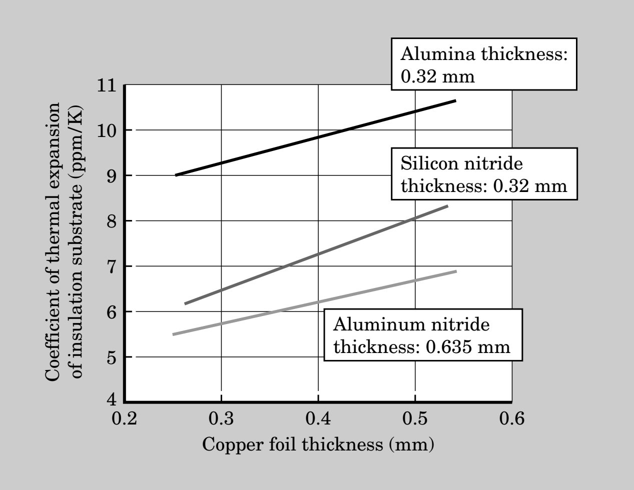

Fig.13 Relationship between the number of thermal cycling tests and solder crack length

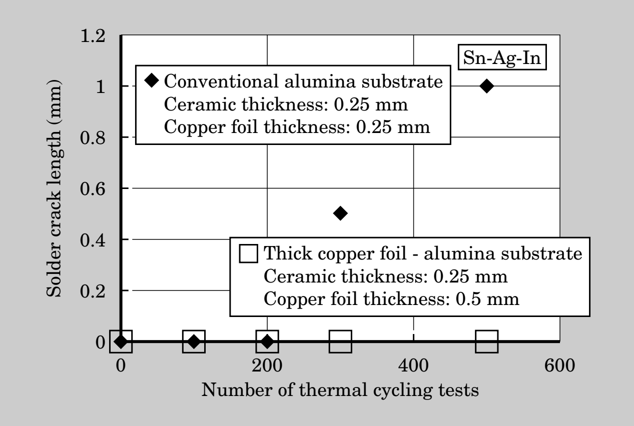

using conventional leaded solder.

6. Higher Reliability with a Thick Copper Foil and Alumina Substrate

To increase reliability even further, we considered making the thermal expansion coefficient of the ceramic insulated substrate approach that of the metal base. Figure 12 shows the results of FEM (finite element method) analysis of the thermal expansion coefficients of various ceramic insulated substrates when the copper foil thickness is changed. It can be seen that the thermal expansion coefficient of the ceramic insulated substrate increases when a thick copper foil base is used.

Fig.14 Alumina DCB substrate cross-sections

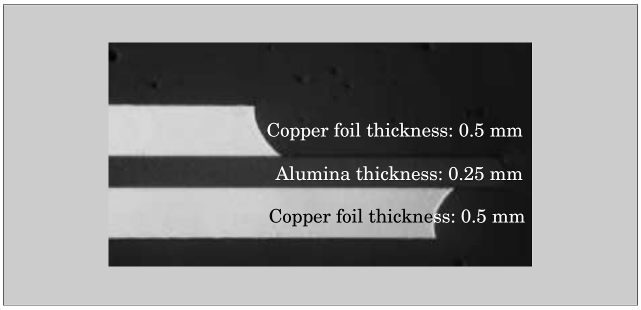

Using an insulated substrate having an alumina ceramic thickness of 0.25 mm and various thicknesses of copper foil, we investigated the amount of deformation in the metal base. By increasing the copper foil thickness from 0.25 mm to 0.5 mm, the amount of deformation of the metal base could be reduced by approximately 100 µm. From this result, it is understood that increasing the thickness of the copper foil actually increases the thermal expansion coefficient of the ceramic insulated substrate.

We conducted thermal cycling tests on samples having an insulated substrate and thicker copper foil (Fig. 13). In a sample having a copper foil thickness of 0.25 mm, cracks occurred after 300 thermal cycles. By changing the copper foil thickness to 0.5 mm, no cracks occurred even after 500 thermal cycles. Increasing the thickness of the copper foil successfully suppressed the progress of cracks in the thermal cycle tests. Figure 14 shows cross-sections of alumina DCB (direct copper bonding) substrates in which an alumina ceramic is joined to a 0.5 mm-thick copper foil.

Furthermore, it has been shown that the use of thicker copper foil also improves the thermal resistance. Even in a structure equipped with a metal base, by increasing the thickness of the copper foil from 0.25 mm to 0.5 mm, we succeeded in decreasing the thermal resistance by approximately 15 %.

7. Conclusion

Fuji Electric has established lead-free IGBT module technology that uses an alumina ceramic insulated substrate and Sn-Ag-In solder to achieve better ability to withstand thermal cycle testing than when Sn-Ag solder is used. Moreover, by using an alumina ceramic insulated substrate and thicker copper foil, lower thermal resistance and high-reliability, even with lead-free solder, can be achieved.

Fuji Electric is committed to contributing to the protection of the global environment by developing lead-free IGBT modules that use this technology into commercial products.

References

(1) Morozumi, A. et al. Reliability of Power Cycling for IGBT Power Semiconductor Modules. IEEE Transactions On Industry Applications. vol.39, no.3, 2003-05/06, p.665-671.

(2) Nishimura, Y. et al. New generation metal base free IGBT module structure with low thermal resistance. in Proc. 16th ISPSD. 2004, p.347-350.

Micro DC-DC Converter

Isao Sano
Zenchi Hayashi
Masaharu Edo

1. Introduction

Portable electronic equipment is increasingly requested to provide the apparently conflicting properties of smaller size and greater multi-functionality. Moreover, operation at lower current is also requested in order to reduce power consumption and to extend the duration of continuous battery-powered operation.

The LSI (large scale integrated) circuits used in portable electronic equipment are fabricated with miniaturization processes to run on lower supply voltages, and the power supplies of equipment having just a single Li-ion battery cell (3.6 V) as well as equipment containing two cells (7.2 V) are transitioning from a configuration of a conventional LDO (low drop out regulator) entity toward a configuration based on a DC-DC converter.

So that the battery operation time may be extended as much as possible, power management for the power supply system is needed to turn the power on and off accurately for each LSI circuit acting as a load. For this purpose, a DC-DC converter is required for each power supply to be turned on and off. However, the attachment of a large-size inductor to each DC-DC converter prevents the set from being made smaller and thinner. Moreover, the use of a small-size inductor requires a control IC that operates at high switching frequencies.

This paper describes Fuji Electric's FB6800 series of micro DC-DC converters that integrate a control IC and an inductor, having been developed and commercialized in response to the above-described marketplace requirements of portable electronic equipment.

2. Features

As can be seen in Table 1, the FB6800 series consists of seven types of micro DC-DC converter products that combine an inductor and a control IC which implements buck, boost, or inverted boost voltage conversions.

As shown in Fig. 1, the inductor area of the micro DC-DC converter is fabricated by plating wiring on a ferrite base, and at the same time, pad electrodes necessary for mounting are also formed. The electrode area of the control IC is ultrasonically flip-chip bonded to an inductor.

Table 1 FB6800 series of micro DC-DC converters

Model	Conversion method	Output voltage	Maximum output current	Synchronous/asynchronous	Example applications
FB6813Q	Buck	1.05 to 2.025 V	300 mA	Synchronous rectification	CPU
FB6804Q	Buck	2.5 to 5.15 V	300 mA	Synchronous rectification	I/O
FB6824Q	Buck	2.5 to 5.15 V	300 mA	Asynchronous	I/O
FB6805Q	Buck	3.0 to 3.45 V	600 mA	Synchronous rectification	Motor
FB6825Q	Buck	3.0 to 3.45 V	600 mA	Asynchronous	Motor
FB6806Q	Boost	15.5 to 16.25 V	40 mA	Asynchronous	CCD
FB6807Q	Inverted boost	– 27.0 V input voltage	20 mA	Asynchronous	White LED

Fig.1 Ultrasonic flip-chip bonding

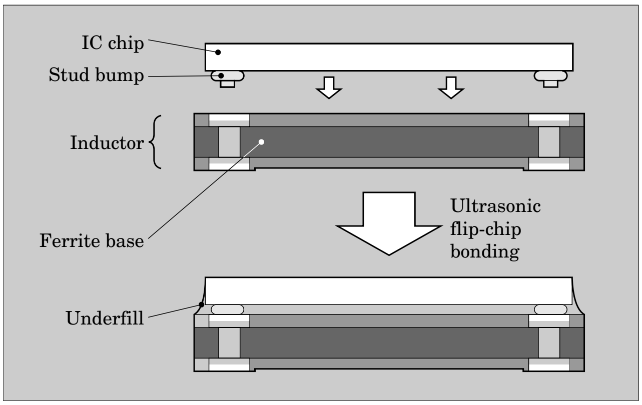

Main features are described below.

(1) External shape

The dimensions of the micro DC-DC converter shown in Fig. 2 are 3.5 mm × 3.5 mm, with a maximum thickness of 1 mm.

(2) Package

As shown in Fig. 3, the use of a 12-pin CSM (chip size module) enables the micro DC-DC converter module to be realized at nearly the same size as the chip itself.

(3) Terminal configuration

The terminal area is configured with an LGA (land grid array) that is not exposed to the package exterior, and which enables the smaller required mounting area.

(4) Inductor: $L = 1.64\ \mu\text{H}$ (300 mA), $R_{\text{dc}} = 0.2\ \Omega$

Ferrite was selected as the base material in order to reduce core loss, and the design was optimized to impede magnetic saturation.

(5) Input voltage

In order to realize high efficiency with a relatively high voltage of 4 to 8.4 V (corresponding to two Li-ion battery cells), an LDD (lightly doped drain) CMOS (complementary metal oxide semiconductor) structure was used and the LDD ion implantation density and dimensions were optimized.

(6) Protection circuit

A protection circuit is built-in to protect against such abnormal conditions as an output short to ground, chip overheating, and UVLO (under voltage lock out), etc. If an abnormal condition is detected, operation is stopped. Setting of the ALERT pin to Low-level releases the protection state, and setting it to High-level restores the protection state.

Fig.2 Appearance of micro DC-DC converter (1)

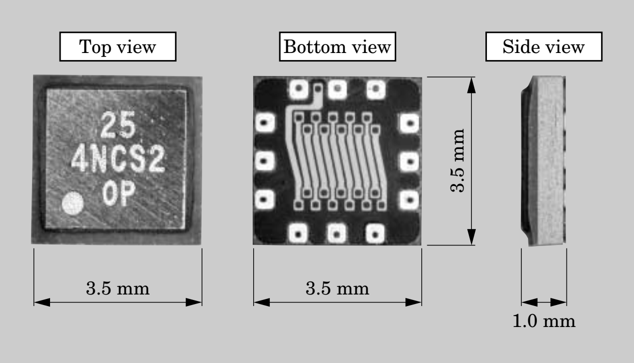

Fig.3 Appearance of micro DC-DC converter (2)

(7) Switching frequency: 2 MHz

High-speed operation is realized with a design in which the dead time control, driver circuits, high-speed comparator and oscillation circuit were optimized.

(8) Serial interface

A serial interface with the CPU enables the implementation of various settings such as ON/OFF of the power supply operation, output voltage settings, and the like.

(9) Soft-start operation with no time lag

By providing an offset voltage at the input to the comparator for soft-start, the time delay from the receipt of an ON-signal until the start of switching has been reduced.

(10) Low current consumption: 1 µA during standby, 800 µA during operation

Each circuit block has been designed to consume less current so that the portable electronic equipment can realize the necessary lower current consumption.

Main electrical characteristics of the FB6813Q are listed in Table 2.

3. Micro DC-DC Converter Module Technology

The micro DC-DC converter assembly utilizes flip-chip bonding.

With an assembly that uses conventional wire bonding, wires extend from the chip to the wire-connecting base, and as a result the inductor becomes larger in size and impedes efforts to save space.

With flip-chip bonding, instead of using wires, stud electrodes known as bumps are fabricated on the IC chip surface for the purpose of forming connections, and are directly mounted to the inductor base.

Bumps are fabricated using wire bonding to form stud bumps as shown in Fig. 4. To fabricate a bump, a gold ball is formed at the tip of a gold wire, that gold

Fig.4 Stud bump photograph

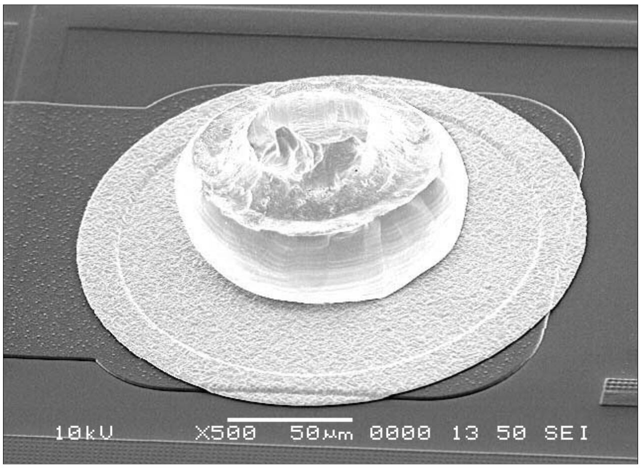

Table 2 Main electrical characteristics of the FB6813Q

Item	Symbol	Condition	Min.	Typ.	Max.	Unit
Power supply voltage	V_{IN}	—	3.0	—	8.4	V
Control power supply voltage	V_{DD}	—	2.93	3.0	3.07	V
Output voltage	V_{OUT}	SEL = H, SD = 0010, No load	1.029	1.05	1.071	V
		SEL = H, SD = 0000, No load	1.078	1.10	1.122	V
		SEL = H, SD = 0001, No load	1.127	1.15	1.173	V
		SEL = H, SD = 1000, No load	1.176	1.20	1.224	V
		SEL = H, SD = 1001, No load	1.225	1.25	1.275	V
		SEL = H, SD = 1010, No load	1.274	1.30	1.326	V
		SEL = H, SD = 1011, No load	1.323	1.35	1.377	V
		SEL = H, SD = 0100, No load	1.47	1.50	1.53	V
		SEL = H, SD = 0101, No load	1.519	1.55	1.581	V
		SEL = H, SD = 0110, No load	1.568	1.60	1.632	V
		SEL = H, SD = 0111, No load	1.617	1.65	1.683	V
		SEL = H, SD = 0011, No load	1.666	1.70	1.734	V
		SEL = H, SD = 1100, No load	1.764	1.80	1.836	V
		SEL = H, SD = 1101, No load	1.837	1.875	1.913	V
		SEL = H, SD = 1110, No load	1.911	1.95	1.989	V
		SEL = H, SD = 1111, No load	1.984	2.025	2.066	V
Efficiency	η	V_{IN} = 3.6 V, V_{OUT} = 1.8 V, I_{OUT} = 0.2 A	85	89	—	%
Line regulation	$\Delta V_{OUT}/V_{IN}$	V_{IN} = 4 to 8.4 V, V_{OUT} = 1.5 V, I_{OUT} = 0.3 A	0	—	±1	%
Load regulation	$\Delta V_{OUT}/I_{OUT}$	V_{OUT} = 1.5 V, I_{OUT} = 0 to 0.3 A	0	—	±0.04	mV/mA
Open loop voltage gain	A_V	—	60	—	—	dB
Unity gain bandwidth	f_T	—	1	—	—	MHz
Overheat protection temperature	T_{SD}	—	125	—	150	°C
Oscillation frequency	f_{osc}	—	1.8	2.0	2.2	MHz
Current consumption	I_{VDD}	VDD pin, when off	—	—	1.0	µA
		VDD pin, during operation	—	—	800	µA
	I_{PVDD}	PVDD pin, when off	—	—	1.0	µA

ball is then bonded to an electrode on the IC chip, leveling is performed to align the bump height, and then the wire is cut.

Gold plated electrodes are also fabricated on the surface of the inductor base, and are bonded to the control IC with ultrasonic Au-Au bonding.

Next, the gap between the flip-chip bonded inductor and control IC is coated and filled with underfill material to ensure the bonding strength, and finally the inductor base is diced to form individual micro DC-DC converter chips.

4. Application Circuit

Figure 5 shows a block diagram and Fig. 6 shows an example application circuit of the FB6813Q. This product contains a built-in inductor and output MOS (metal oxide semiconductor), and therefore enables a buck switching power supply to be configured simply with input and output capacitors, and a phase compensation capacitance and resistance as the only external components, thus contributing to space savings of the set.

The following improvements were implemented to realize high efficiency in the FB6813Q.

(1) Control circuit: Dead time control, and lower current consumption and optimization of the oscillation frequency for each block
(2) Output MOS: Optimized high-voltage design for low on-resistance and low gate charge
(3) Inductor: Selection of base material that reduces core loss

After implementing the abovementioned improvements, efficiency was measured when the load and output voltage are changed, and as shown in the example of Fig. 7, a high efficiency of 90 % was realized with an input voltage (V_{IN}) of 3.6 V, an output voltage (V_{OUT}) of 1.8 V and an output current (I_{OUT}) of 180 mA.

By using the newly developed FB6800 series of products, a micro DC-DC converter can be installed in the vicinity of a device acting as a load and a micro processor can implement serial control to turn the power supply on and off, thus enabling the set to be made smaller, thinner, and a distributed system to be

Fig.5 FB6813Q block diagram

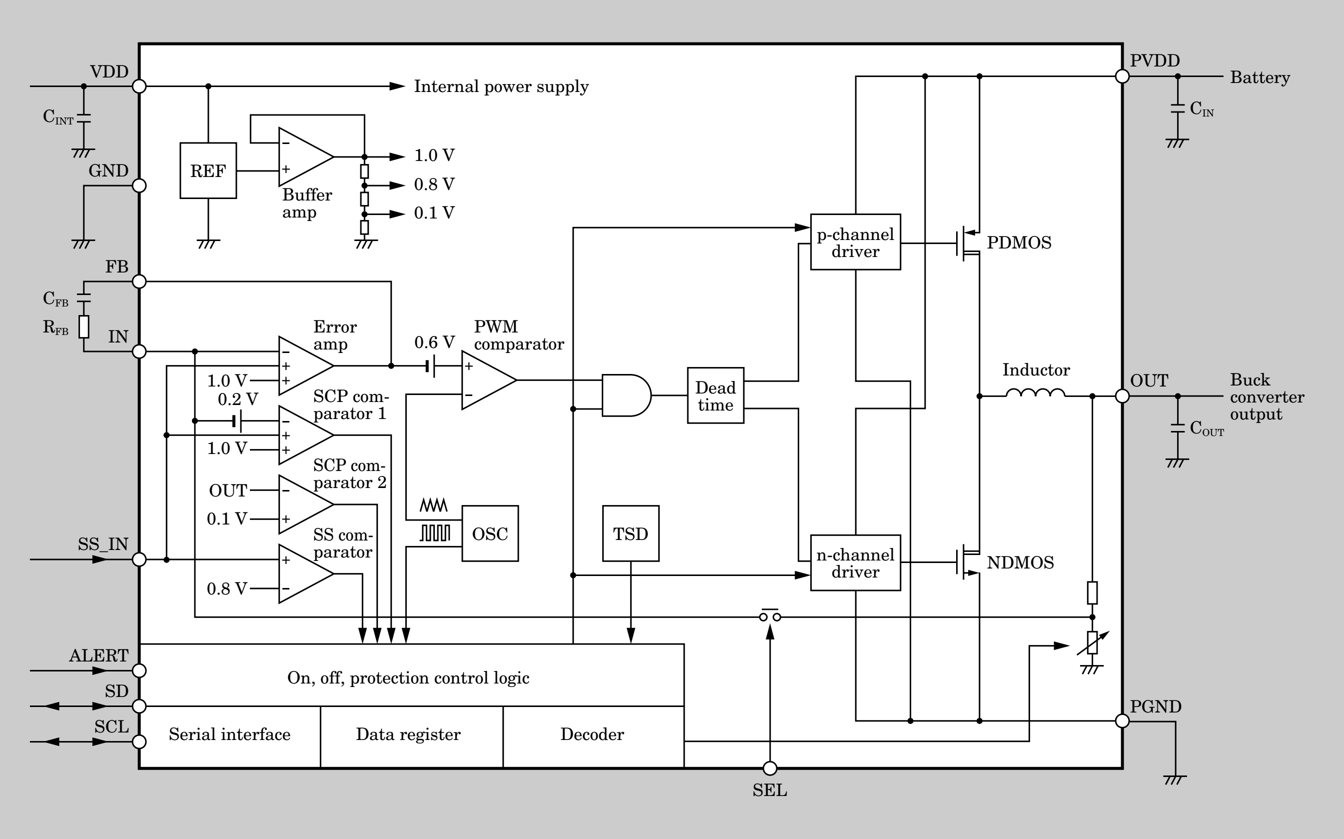

Fig.6 Example of FB6813Q application circuit

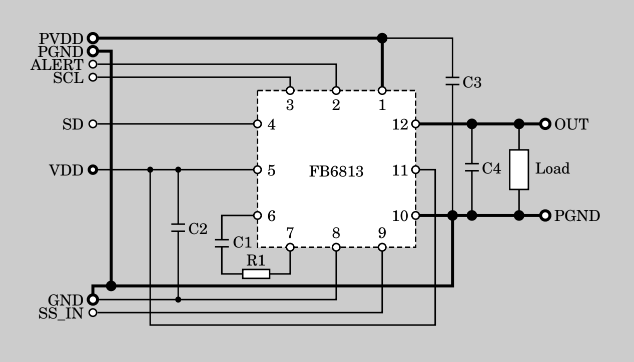

Fig.7 Example of measured efficiency of the FB6813Q

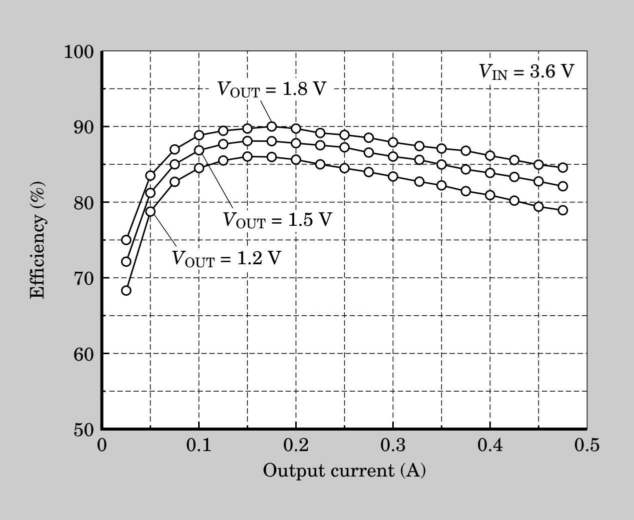

configured that achieves longer battery life.

5. Conclusion

The FB6800 series of micro DC-DC converters developed mainly for applications in DVCs (digital video cameras) and DSCs (digital still cameras) has been introduced.

In the future, Fuji Electric intends to broaden the product line by adding a micro DC-DC converter for a single Li-ion battery cell as used in cellular phones and DSCs, while at the same time, striving to realize higher efficiency and smaller size.

Reference

(1) Hayashi, Z. et al. High-Efficiency DC-DC Converter Chip Size Module with Integrated Soft Ferrite. The 2003 International Magnetics Conference (INTERMAG 2003).

Two-channel Current Mode Synchronous Buck Regulator Control IC

Akira Nakamori
Tomomi Nonaka
Akira Ichioka

1. Introduction

Recently, digital home appliances such as digital televisions, DVD (digital versatile disk) players and DSCs (digital still cameras) have grown in popularity. In particular, in Japan, the transition to digital terrestrial broadcasting which began in 2003 is expected to be complete for all television broadcasts by 2011.

This paper introduces Fuji Electric's FA7731F, a 2-channel current mode synchronous buck regulator control IC developed for use with a CPU as a power supply for the tuner unit in digital televisions, which are rapidly growing in popularity.

2. Product Overview

Figure 1 shows the appearance of Fuji Electric's newly developed and commercialized power supply control IC.

2.1 IC features

In order to build digital television tuners that are more compact in size and less expensive, even the power supply system is increasingly being required to use fewer parts, dissipate less power, and to be less expensive. In digital television tuner applications, in order to supply a low-voltage and high-current to the CPU (acting as a load) from a relatively high voltage of approximately 7 to 14 V, a synchronous buck regulator control IC that has a large power dissipation capacity and contains a high-voltage low on-resistance output MOSFET (metal oxide semiconductor field-effect transistor) is needed. However, since no IC on the market has specifications that meet such requirements, Fuji Electric took the initiative to lead its competitors and develop such a commercial IC.

Fig.1 Appearance of the FA7731F

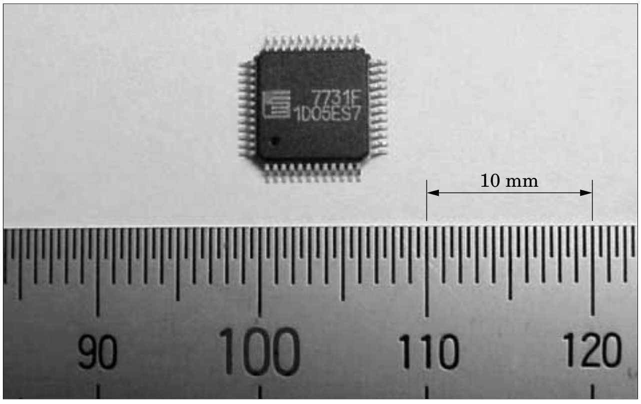

The features of this IC are described below. Firstly, it has excellent high-speed response to fluctuations in the load. The CPU, acting as a load, causes large fluctuates in the load, and a current mode control system and a synchronous rectification output system are used to suppress those fluctuations instantaneously. Secondly, it is compact. To realize a more compact size of the power supply, four power MOSFETs for two channels are all integrated into the power supply control IC. Thirdly, it is inexpensive. An output voltage detection resistor and a feedback resistor and capacitor for an error amplifier, which were previously attached externally, have also been integrated into the power supply control IC.

The IC is housed in a compact, thin and high-power dissipating TQFP48 pin (exposed pad) package. Specifications of the power supply control IC are listed in Table 1.

2.2 Operation

Figure 2 shows the circuit block diagram of the FA7731F. The operation of each circuit block is described below.

(1) ON_OFF circuit

The entire power supply can be controlled to turn on or off by switching the ON_OFF pin. When turned off, the current consumption of the power supply control IC is 8 µA, and a standby current can be realized.

(2) Oscillator circuit

The oscillation frequency of the power supply control IC is set to an arbitrary frequency between 100 and 400 kHz by connecting a resistor ranging from 18 to 82 kΩ between the RT pin and ground. The phase difference between the frequencies of channels 1 and 2 is 180 degrees. As a result, the size of the input capacitor can be reduced.

Table 1 Specifications of the FA7731F

Input voltage		7 to 14 V
Output voltage		≥1 V
No. of output channels		2
Switching control system		Current mode
Switching frequency		100 to 400 kHz
Rectification system		Synchronous rectification with internal output power MOSFETs
Phase difference between channels		180 degrees
Slope compensation		Adjusted with external resistor
Operation mode control	ON/OFF control	Switches ON/OFF entire power supply
	CS1 control	Switches ON/OFF channel 1
	CS2 control	Switches ON/OFF channel 2
Compensation parts for error amplifier	Internal	Built-in
	External	Can be attached to FB pin
Voltage detection	Internal	1.5 V (switched by SEL pin)
		1.2 V (switched by SEL pin)
	External	Arbitrary (switched by SEL pin)
Protection function	Soft-start	Adjusted with external capacitor
	Timer latch	Adjusted with external capacitor
	UVLO	6.5 V (on), 6.0 V (off)
	Overcurrent protection	4.5 A
	Overheat protection	145°C
Package		TQFP48 pin (exposed pad) ($\theta_{\text{j-a}}$ = 25.9°C)

Fig.2 Circuit block diagram

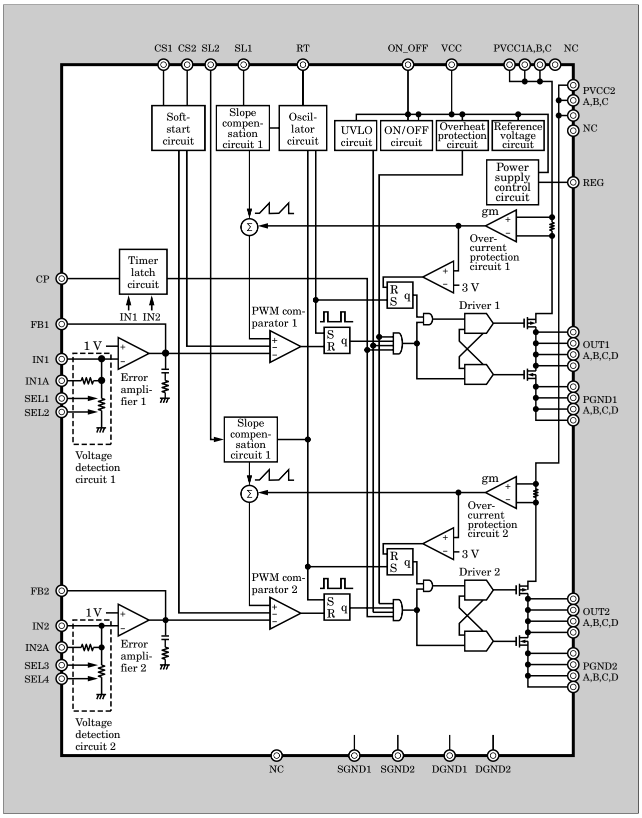

Table 2 SEL pin vs. output voltage

Channel	Output voltage	SEL1	SEL2	SEL3	SEL4
1	Arbitrary	Ground	Open		
	1.5 V	Ground	Ground		
	1.2 V	Open	Ground		
2	Arbitrary			Ground	Open
	1.5 V			Ground	Ground
	1.2 V			Open	Ground

(3) Slope compensation circuit

With peak current mode PWM (pulse width modulation) control, subharmonic oscillation may occur at duty cycles of 50 % or above. In order to avoid this phenomenon, SL pins are provided separately for channel 1 and channel 2. By connecting a resistor of 10 to 50 kΩ between the SL pin and ground, a compensating signal is automatically generated inside the IC and subharmonic oscillation can be avoided.

(4) Soft-start circuit

Each channel is provided with a soft-start circuit. An internal current source is built into the CS pin, enabling the soft-start period of the power supply to be adjusted by changing the value of an external capacitor.

(5) Timer-latch short-circuit protection circuit

This circuit monitors the input voltages to the error amplifier of each channel, and if a state in which the input voltage to either channel is 0.2 V lower than the usual voltage (1.0 V) continues for the duration of time that exceeds the setting period of the timer latch circuit, the driver outputs of both channels are stopped simultaneously. Similar to the CS pin, the CP pin also contains an internal current source and the timer latch setting time can be adjusted to an arbitrary value by changing the value of an external capacitor.

(6) Overheat protection circuit

If the IC temperature is at least 145°C for a duration of time that exceeds the setting period of the timer latch circuit, the overheat protection circuit stops the driver outputs of both channels simultaneously.

(7) Undervoltage lockout (UVLO) protection circuit

If the supply voltage (VCC) drops to 6.0 V or less, this protection circuit stops the driver outputs of both channels simultaneously. If VCC recovers to a voltage of at least 6.5 V, the power supply is automatically restored.

(8) Pulse-by-pulse overcurrent protection circuit

This circuit monitors the current flowing to the main MOSFET in each channel, and if that current increases to 4.5 A or above, turns off the main MOS

FET and provides a pulse-by-pulse overcurrent function.

(9) Output voltage detection circuit

The output voltage detection circuit is capable of switching between three modes by switching the four SEL pins (SEL1 to SEL4). Table 2 lists the correspondence between the SEL pins and output voltage. Detection of the output voltages of 1.2 V and 1.5 V is implemented using the IC's internal detection resistor. A mode for detecting arbitrary voltages is supported with externally attached detection resistors.

(10) Setting pin for feedback resistor and capacitor of error amplifier

Compensation parts for the error amplifier are built-in, thus simplifying the design of the power supply. The compensation provided by these built-in parts can be changed by adding capacitance and resistance in series between the FB pin and ground.

3. Application Circuit

3.1 Circuit configuration

Figure 3 shows an example application circuit for the FA7731F. In this example, the supply voltage is 9 V, the channel 1 output is 1.2 V and the channel 2 output is 1.5 V. There are a total of nine externally connected chip capacitor and chip resistor parts, and since the power MOSFET is integrated inside the IC instead of connected externally as in the past, the circuit configuration is extremely compact and simple.

Fig.3 Application circuit example

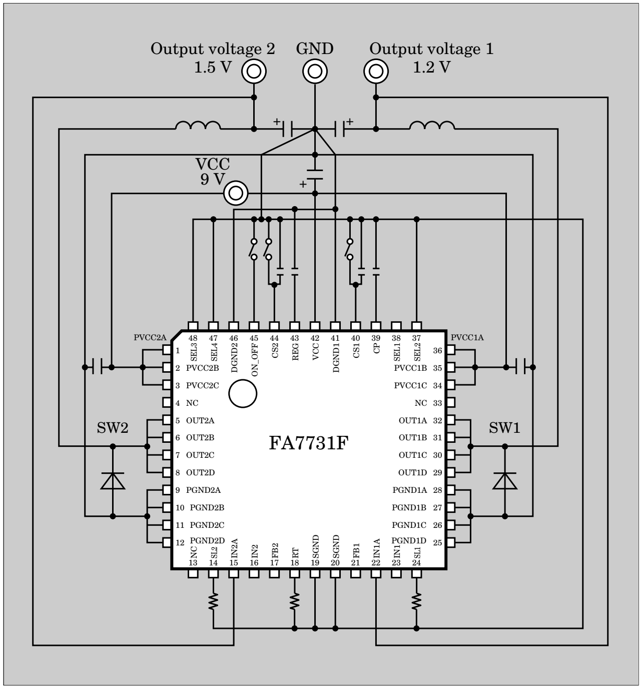

Table 3 ON resistance of internal power MOSFETs

Channel	Device	ON-resistance (Ω)
1	PMOSFET	0.3
	NMOSFET	0.2
2	PMOSFET	0.4
	NMOSFET	0.1

3.2 Efficiency characteristic

The output power MOSFETs of both channels are configured as synchronous rectification systems in order to increase efficiency. Table 3 lists the on-resistance of the internal power MOSFETs of each channel. Figure 4 shows the efficiency characteristic of channel 1 when channel 2 switching has been stopped. Similarly, Fig. 5 shows the efficiency characteristic of channel 2 when channel 1 switching has been stopped. Figures 4 and 5 show that efficiency of greater than 90 % can be obtained when the output voltage is 5 V.

Fig.4 Efficiency of output voltage 1

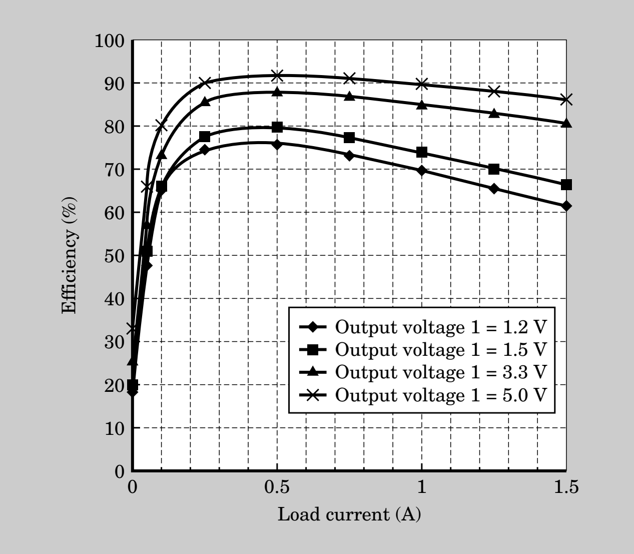

Fig.5 Efficiency of output voltage 2

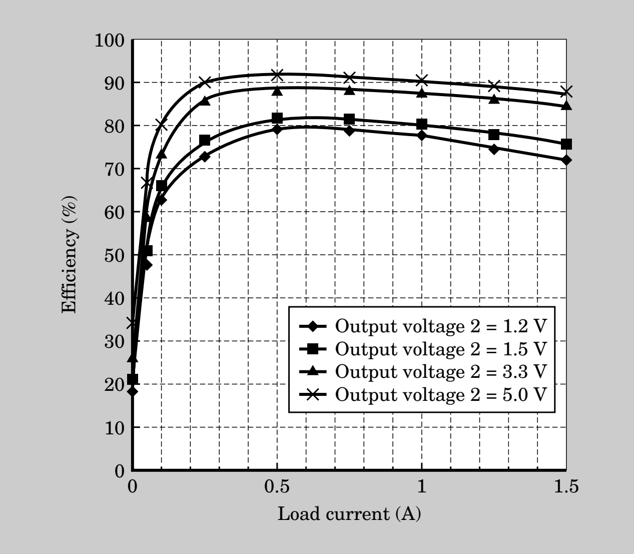

Fig.6 Drain-to-source voltage waveforms of synchronous rectification-side MOSFETs

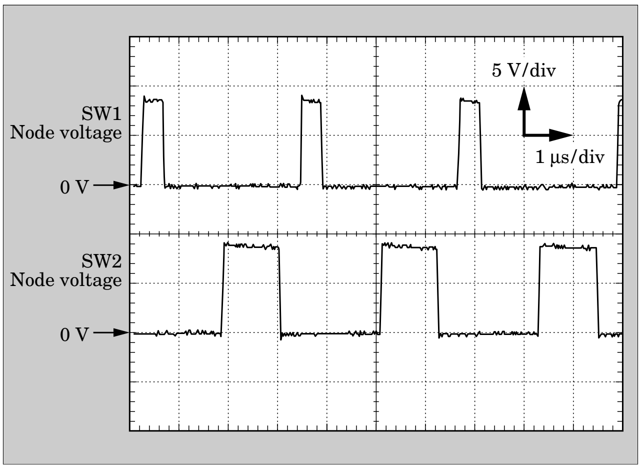

Fig.7 Steady state output voltage waveforms when output voltage is set to 1.0 V

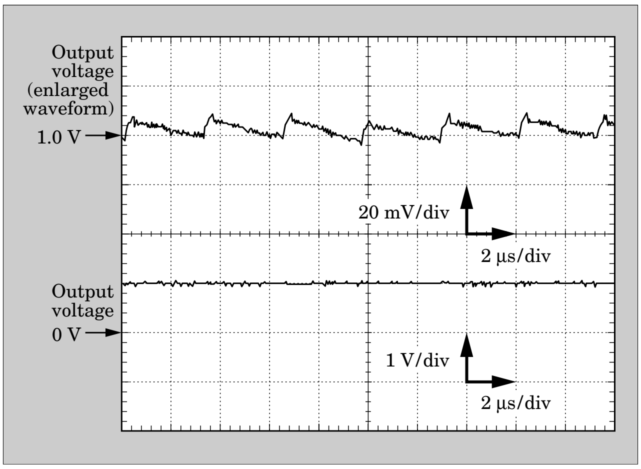

Fig.8 Transient state output voltage waveforms in response to 1 A load fluctuations when output voltage is set to 1.2 V

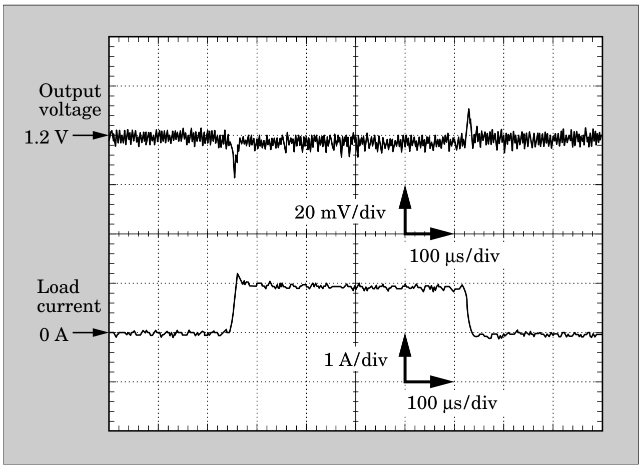

3.3 Two-phase operation

Both channels have the same frequency, but their phases differ by 180 degrees. Figure 6 shows the drain-to-source voltage waveforms of synchronous rectification-side MOSFETs when both channels are operating. From Fig. 6 it can be seen that by shifting the operation of both channels by 180 degrees, the peak input ripple current is reduced to half the value of the peak current during synchronous operation, and the RMS current of the input capacitor is reduced drastically, thereby enabling the size of the input capacitor to be reduced.

3.4 Characteristic of low output voltage

Output voltage detection has two modes, an external mode and an internal mode. In the case of the internal mode, the lowest output voltage is 1.2 V. In the case where use of an even lower voltage is desired, by configuring the SEL pins to set the voltage detection resistor to external mode and setting the externally attached voltage detection resistor to an appropriate value, the output voltage can be adjusted to any arbitrary value of 1.0 V and above. Figure 7 shows the steady state output voltage waveforms when input voltage and output voltage are set to 9.0 V and 1.0 V respectively.

3.5 Characteristic when load fluctuates

In order to provide stable supply voltage, the DC-DC converter control system employs a current mode system having excellent stability. Figure 8 shows the transient state output voltage waveforms when the output voltage is set to 1.2 V. In response to 1 A step-up and step-down load fluctuations, an excellent transient state characteristic is exhibited with output fluctuations of 20 mV or less and extremely small load fluctuations.

4. Conclusion

This paper has presented an overview of Fuji Electric's 2-channel current mode synchronous buck regulator control IC that contains built-in power MOSFETs.

With the rapid proliferation of digital home appliances, the power supplies in those products are increasingly being required to provide higher performance and smaller size, and to be less expensive.

In response to these marketplace requirements, Fuji Electric remains committed to lowering the on-resistance of power MOSFETs, to reducing the part count by eliminating external Schottky barrier diodes and external capacitors such as used in the soft-start and timer latch circuits, and to raising the quality of and providing more compact and less expensive power supplies.

Reference

(1) Middlebrook, R. D. Topics in Multiple-Loop Regulators and Current-Mode Programming. IEEE Transactions on Power Electronics. vol.PE-2, no.2, 1987-04.

Quasi-resonant Controller IC

Hiroshi Maruyama
Hironobu Shiroyama
Takaaki Uchida

1. Introduction

The problem of global warming has attracted considerable attention in recent years, and requirements for energy savings in all electronic products, and regulations prescribing the amount of standby power per product type and the like are becoming more and more severe with each passing year.

Under these circumstances, Fuji Electric has developed energy-saving AC-DC converter switching mode power supply controller ICs for converting an AC line input voltage (100 V, 240 V AC) to a DC voltage. Among these ICs, Fuji has moved ahead with the commercialization of a control IC that is effective in reducing the standby power in an internal high-voltage startup current source, and has developed the FA5516 series of PWM (pulse width modulation) control ICs for fixed frequency operation. These types of ICs contain an internal high-voltage startup current source that functions to supply startup current from a high-voltage input line of 100 to 240 V AC to the VCC pin of the control IC prior to switching, and then to stop that startup current when the transformer's secondary side voltage rises after the switching has started. In the past, a startup resistor was used, and startup current flowed continuously while the IC was operating, but with Fuji Electric's newly developed IC, switching can be implemented so that the startup current only flows when necessary.

This paper presents an overview of Fuji Electric's newly developed FA5530 and FA5531 quasi-resonant controller ICs equipped with an internal high-voltage startup current source.

2. Product Overview

2.1 Features

The FA5530 and FA5531 are AC-DC power supply controller ICs developed for switching mode power supplies that use quasi-resonant control. By indirectly sensing the drain voltage of a power MOSFET (metal oxide semiconductor field-effect transistor) via the voltage of an auxiliary winding, and then by turning ON the next cycle at a timing determined by the minimum voltage during resonant operation after the energy stored in the transformer has been supplied to the secondary side, lower switching loss, higher efficiency and lower noise can be achieved more easily, and these ICs are well suited for applications such as power supplies for printers and LCD TVs in which noise has been a problem.

Fig.1 External view of products

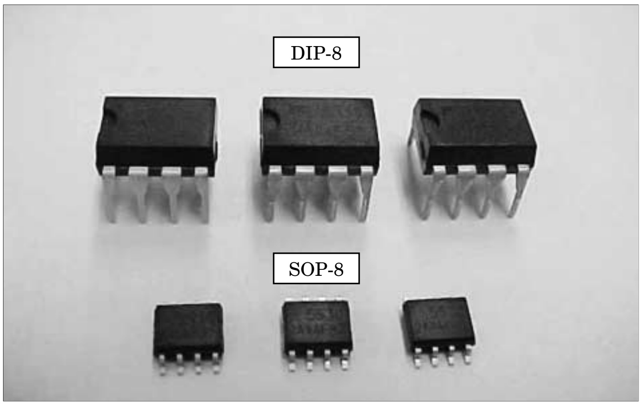

Fig.2 Chip configuration of the FA5531

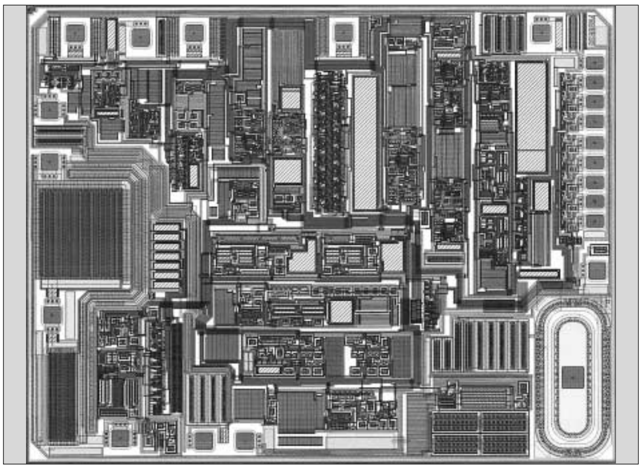

Figure 1 shows an external view of the product packages (DIP-8 and SOP-8), and Fig. 2 shows the chip configuration of the FA5531. Features of the FA5530 and FA5531 ICs are described below.

(1) A 500 V high-voltage JFET (junction field-effect

transistor) is built-in, and the IC supplies or stops the flow of charging current from the VH pin to the capacitor of the VCC pin.

While current is being supplied:

7 to 3.5 mA (V_{CC} = 0 V to UVLO off)

While current is stopped: 20 µA

(2) Quasi-resonant control during operation at a light load causes the switching frequency to increase. But in these ICs, the switching frequency is decreased, by limiting the maximum switching frequency, or by reducing the maximum frequency linearly if the FB pin voltage (feedback voltage from the secondary side) drops below 1.3 V.

Maximum switching frequency: 65 kHz (FA5530)
130 kHz (FA5531)
Minimum switching frequency: 1 kHz
(FA5530, FA5531)

(3) The ZCD pin senses transitions from high to low values of the auxiliary winding voltage. The threshold voltages are V_{HL} = 62 mV and V_{LH} = 152 mV with hysteresis, and the upper and lower limits of the ZCD input voltage are clamped at 9.2 V (I_{zcd} = 3 mA) and – 0.75 V (I_{zcd} = – 2 mA), respectively. Additionally, by externally pulling up the ZCD pin to at least 8 V, latched stopping can be forcibly implemented.

(4) The VCC pin contains a built-in UVLO (undervoltage lockout) circuit having hysteresis.

V_{CC} = 9.85 V when ON, and = 9.10 V when OFF

(5) The IS pin is for sensing the current of an external MOSFET, and the maximum input level is 1 V. In order to prevent malfunctions due to noise when the pin is ON, a blanking time of 380ns is set.

(6) Various protection functions are built-in, including overload protection (auto restart), VCC pin overvoltage protection (latch), soft-start (internally fixed at 1 ms), etc.

(7) The package supports high voltages and is available in two varieties, DIP-8 and SOP-8. The high-voltage startup current source (VH) pin is set to pin 8, and pin 7 remains as a non-connected (NC) pin.

2.2 Operation during light load condition

Figure 3 shows a block diagram of the entire IC.

With quasi-resonant control, the energy stored in the transformer during the power MOSFET's ON period is transferred to the secondary side during the OFF period, and when the release of energy is complete, resonance is initiated between the transformer inductance L and the drain capacitance C, and the voltage oscillates. Utilizing this control, the next cycle turns ON at a timing corresponding to when the drain voltage decreases to its minimum value, and switching is performed when the current flowing through the transformer is zero and when the drain voltage is small, thereby enabling a reduction in switching loss and noise.

Fig.3 Block diagram of the FA5531

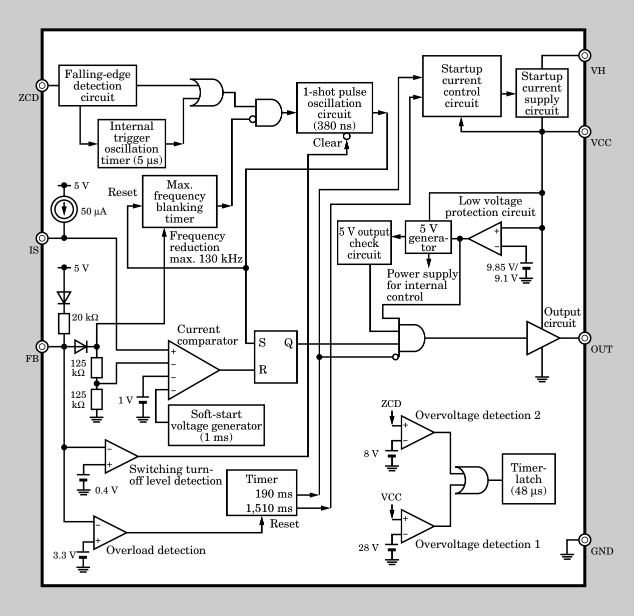

The ZCD pin of Fig. 3 is connected to the auxiliary winding of the transformer through a resistor, and the waveform appearing at this pin has nearly the same shape as the drain waveform of the power MOSFET connected to the primary winding, but has an amplitude that is a fraction of the number of windings and is centered about ground level. The timing at which this waveform falls from a high-level to ground level is sensed, an ON trigger is output (falling edge signal), and adjustment is made so that the cycle turns ON at the actual minimum, taking into account the delay time.

Figure 4 shows the relationship between the load condition (output power P_o) and the switching frequency (f_{sw}) of the power MOSFET, and Fig. 5 shows an image of the change in operating waveforms according to the load condition. When the load is heavy, after the transformer releases its energy, a resonant state is entered and then the next cycle turns ON at the first timing of voltage minimum. At this time, since the ON period and the flyback period during which energy is transferred to the secondary side are both extended, the switching is implemented at a low frequency.

As the load becomes lighter, the abovementioned periods become shorter, and the frequency increases. The FA5531 contains an internal timer (maximum f_{sw} blanking) that counts 7.69 µs (130 kHz) from the ON time, and falling-edge signals are ignored during this period in order to limit the maximum switching frequency to 130 kHz or less.

As the load becomes even lighter, if the voltage of the FB pin that receives the feedback signal from the secondary side drops to 1.3 V or less, the abovementioned maximum frequency limit is decreased linearly, the number of switching operations is reduced, and the

Fig.4 Relationship between output power (load) and switching frequency

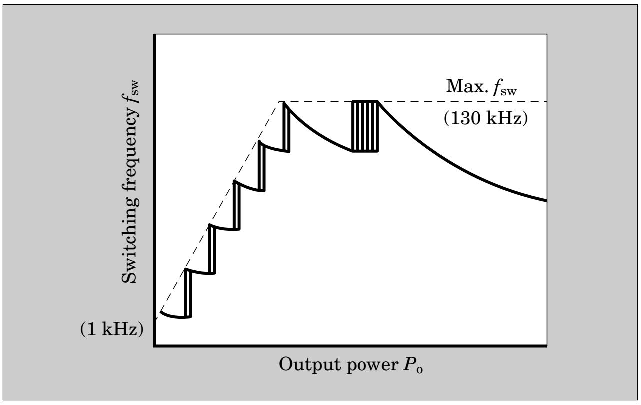

Fig.5 Load condition and operating waveforms

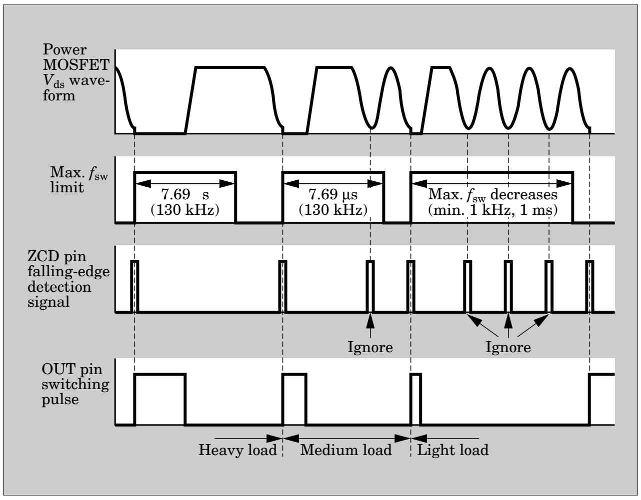

minimum frequency can be lowered down to approximately 1 kHz (See Fig. 4).

2.3 Operation during overload condition

Figure 6 shows waveforms during operation at an overload condition. An overload condition is sensed when the FB pin voltage is 3.3 V or above, and after a delay time of 190 ms following the sensing of the overload condition, the switching is stopped. Consequently, the startup time must be adjusted with smoothing capacitors or the like, provided there are no problems, such that the secondary side rises to its normal value and the FB pin voltage falls within 190 ms. Once an overload stoppage has occurred, the stopped state is maintained for approximately eight periods of 1,510 ms, and then the IC is reset and restarted. During the period while stopped, if the VCC voltage drops down to 9.85 V, the high-voltage startup current source turns ON, the IC repeatedly operates to raise the voltage to 11.55 V with the supply from the VH pin, the startup circuit becomes inoperable after 1,510 ms, and a reset is implemented at the point in time when the VCC pin voltage drops down to the UVLO stop voltage 9.1 V.

Fig.6 Waveforms during an overload condition

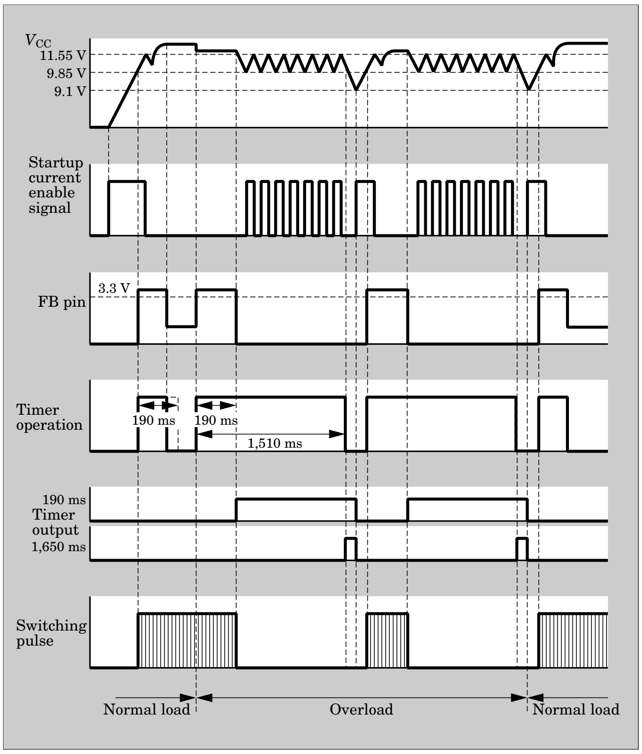

3. Application to Power Supply Circuits

3.1 Power supply for evaluation use

In order to verify the operating characteristic of a power supply circuit that uses this IC, a power supply was built for the purpose of evaluation and its operating characteristics verified (See Fig. 7).

Main specifications of the power supply that was built for the evaluation are listed below:

○ Input line voltage: 80 to 264 V AC, 50/60 Hz
○ Output: 19 V DC, 5 A (95W)
○ Protection functions:
  Overload protection (auto restart), overcurrent control, overvoltage protection (latch)
○ IC used: FA5531 (maximum frequency: 130 kHz)

3.2 Maximum switching frequency limiting

Figure 8 shows the switching waveform at the rated load. From this waveform, it can be seen that turn-ON occurs at the resonance minimum. At this time the switching frequency is approximately 40 kHz.

Figure 9 shows the switching waveform at an approximate 30 % load condition (1.6 A output current). Generally, in the case of quasi-resonant control, the switching frequency increases as the load becomes lighter, but this IC has a function for limiting the maximum frequency, and when the switching frequency reaches its upper limit, the resonance minimum is skipped in order to suppress the increase in switching frequency. In Fig. 9, it can be seen that after one resonance minimum is skipped, an ON region appears

Fig.7 Evaluation SMPS circuit

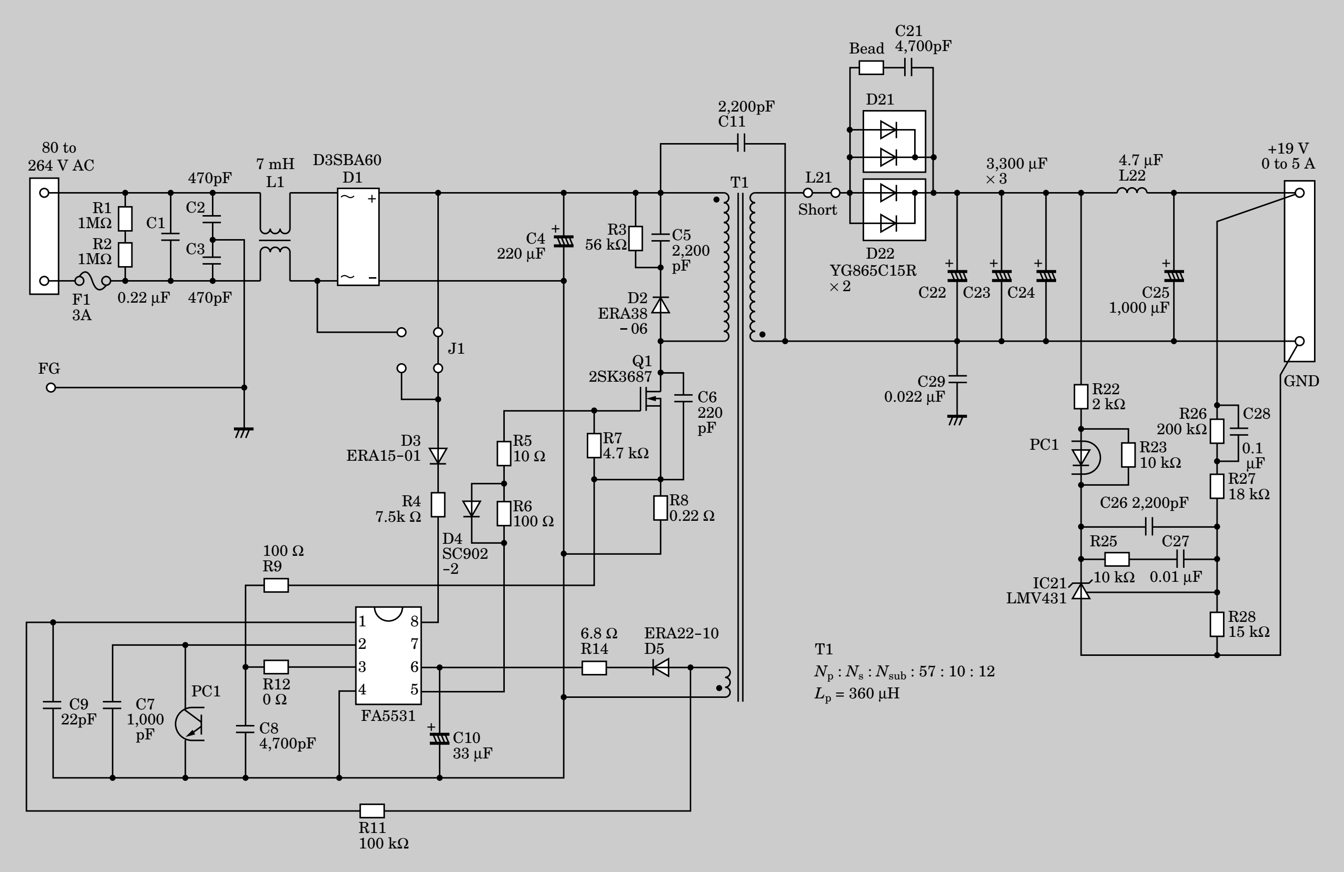

Fig.8 Switching waveform at maximum rated load (100 V AC input)

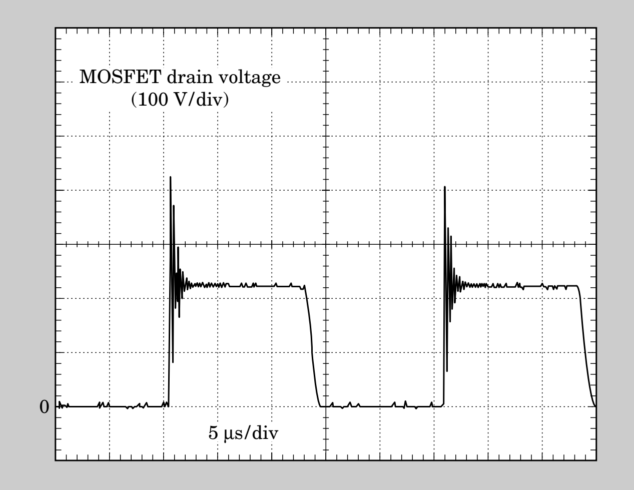

Fig.9 Switching waveform at 30 % load condition (100 V AC input)

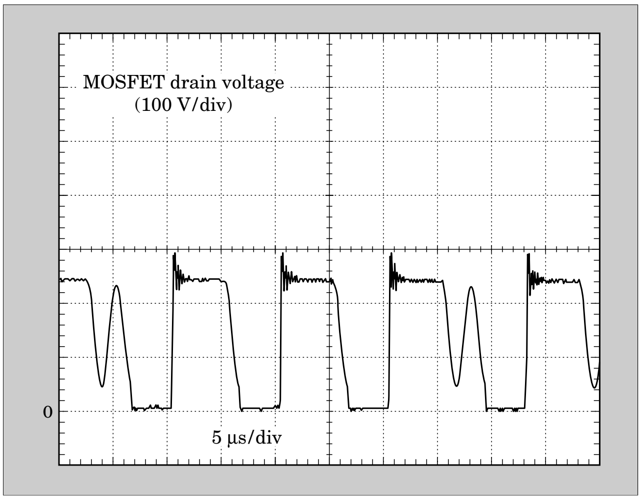

at the second minimum.

Figure 10 shows the change in switching frequency as related to the output current, in the case where clamping was used. From the figure, it can be seen that the switching frequency increases as the output power decreases in the region extending from the rated load to a medium load. On the other hand, it can be seen that the switching frequency decreases as the load becomes lighter in the region extending from a medium load to no load, and that the peak frequency occurs at 100 to 110 kHz.

3.3 Input power at unloaded condition

Power supply circuits used in typical electronic products can be observed operating at an unloaded condition when, for example, an AC adapter is plugged into an electrical outlet but the equipment that utilizes the power does not operate. In this case, since the

Fig.10 Switching frequency characteristics

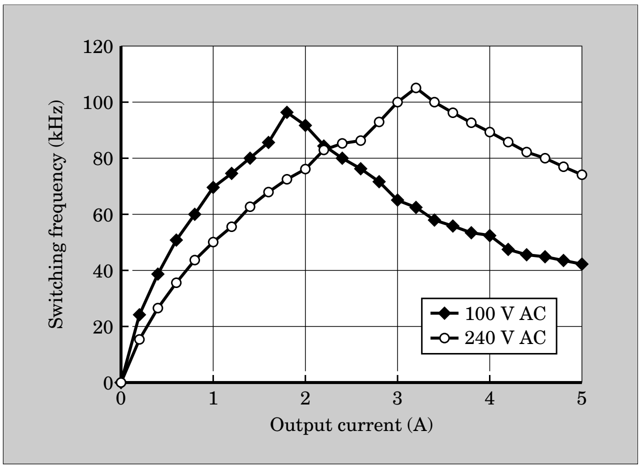

Fig.11 Input power characteristic at unloaded condition

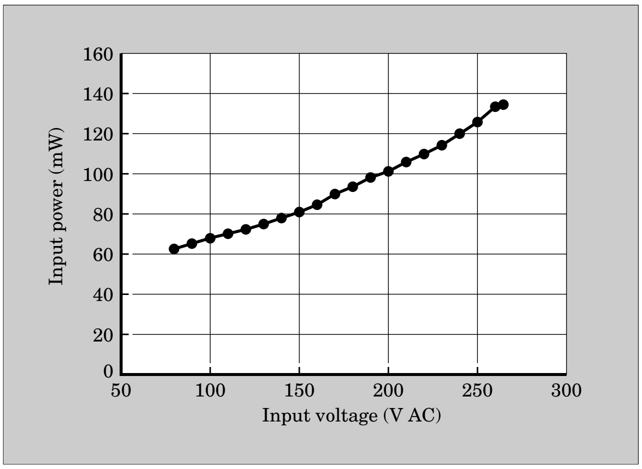

equipment is not operating, all the power input during this unloaded condition is dissipated. From the perspective of energy savings, it is extremely important to reduce the input power during an unloaded condition.

Figure 11 shows the measured input power during unloaded operation with the power supply built for evaluation-use. The input power during unloaded operation of this evaluation-use power supply was suppressed to the low value of 67 mW in the case of 100 V AC, and 120 mW in the case of 240 V AC. Marketplace requirements concerning the input power during unloaded operation vary according to the set of components used, but input power of 300 mW or less is often desired, and the power supply built for evaluation-use achieves this value by a significant margin.

The suppression of input power during unloaded operation to a small value can be attributed to two main factors.

The first factor is the effect of the function for decreasing the switching frequency during operation at a light load. Figure 12 shows the switching waveform during the unloaded operation of this evaluation-use power supply. From this figure, it can be seen that the switching frequency drops to approximately 1 kHz. During unloaded operation or operation at a light load, switching loss can be reduced by decreasing the switching frequency.

Fig.12 Waveform at unloaded condition

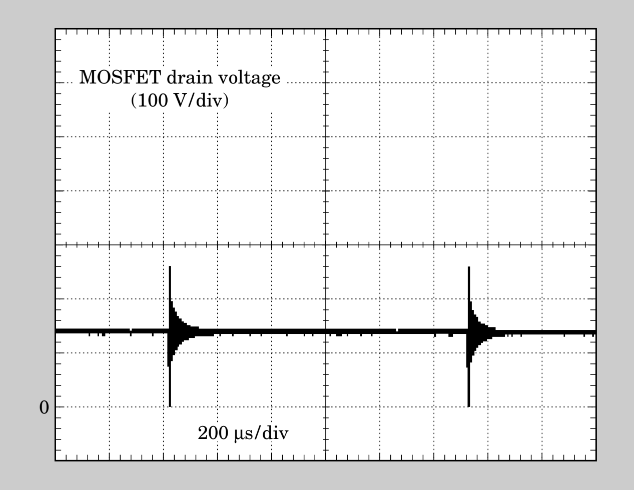

Another factor is the effect of the startup circuit contained inside the IC. In the case of a conventional IC, the startup circuit was configured by attaching an external resistor, and this resistor generated a constant power loss of 100 mW, for example, even after the power supply operation had started. However, because Fuji Electric's newly developed IC contains an internal startup circuit, the power dissipation loss of the startup circuit can be reduced to nearly zero after the power supply has begun operation. This effect enables a reduction in the input power during unloaded operation.

4. Conclusion

An overview of the FA5530 and FA5531 quasi-resonant controller ICs with internal high-voltage startup current source has been presented. Another model, the FA5532 overload latch lockout IC is currently underdevelopment for addition to this series of ICs.

The functions essential for realizing lower standby power consumption in controller ICs equipped with an internal startup current source, without increasing the part count, have been envisioned and Fuji Electric remains committed to advancing and enhancing its series of ICs to meet the needs of various future requirements.

Global Network

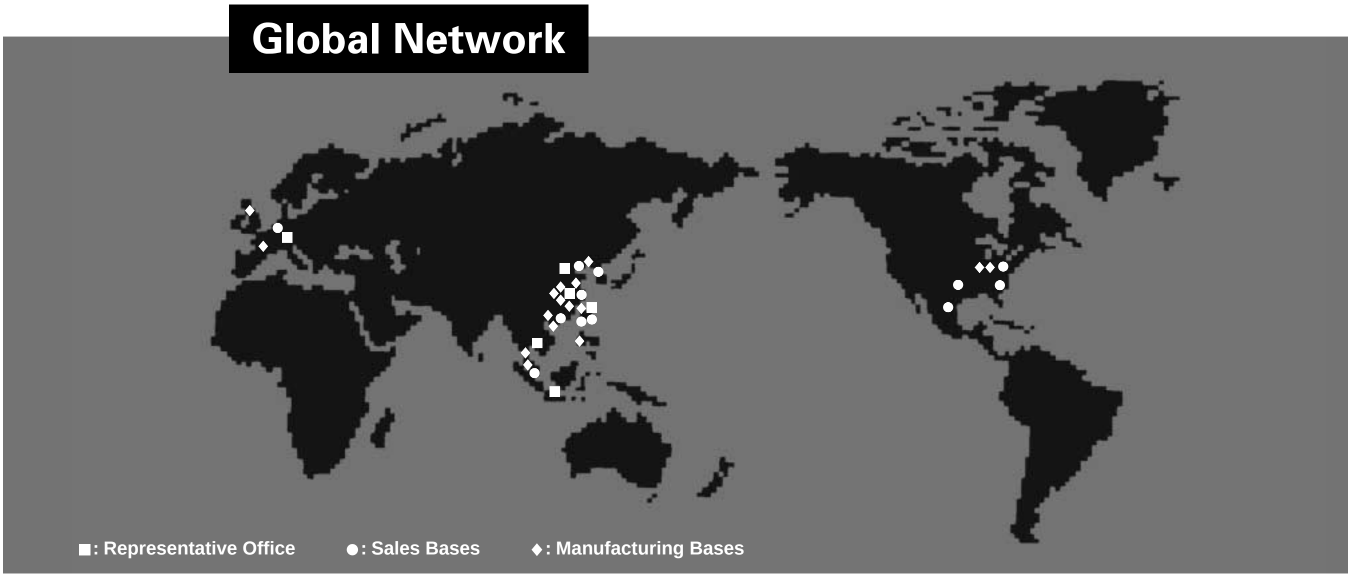

AMERICA

● **FUJI ELECTRIC CORP. OF AMERICA**
USA
Tel : +1-201-712-0555 Fax : +1-201-368-8258

◆ **U.S. FUJI ELECTRIC INC.**
USA
Tel : +1-732-560-9410 Fax : +1-732-457-0042

◆ **FUJI HI-TECH, INC.**
USA
Tel : +1-510-651-0811 Fax : +1-510-651-9070

● **FUJI SEMICONDUCTOR, INC.**
USA
Tel : +1-972-733-1700 Fax : +1-972-381-9991

● **GE FUJI DRIVES, USA INC.**
USA
Tel : +1-540-387-7829 Fax : +1-540-387-8580

● **GE FUJI DRIVES AMERICA S.A. de C.V.**
MEXICO
Tel : +52-8-154-7000 Fax : +52-8-154-7007

EU

■ **FUJI ELECTRIC HOLDINGS CO., LTD.**
Erlangen Representative Office
GERMANY
Tel : +49-9131-729613 Fax : +49-9131-28831

● **FUJI ELECTRIC FA EUROPE GmbH**
GERMANY
Tel : +49-69-6690290 Fax : +49-69-6661020

● **FUJI ELECTRIC DEVICE TECHNOLOGY EUROPE GmbH**
GERMANY
Tel : +49-69-6690290 Fax : +49-69-6661020

◆ **FUJI ELECTRIC (SCOTLAND) LTD.**
U.K.
Tel : +44-1355-234111 Fax : +44-1355-238810

◆ **FUJI ELECTRIC FRANCE S.A.**
FRANCE
Tel : +33-4-73-98-26-98 Fax : +33-4-73-98-26-99

ASIA

East Asia

■ **FUJI ELECTRIC HOLDINGS CO., LTD.**
China Representative Office (Shanghai)
CHINA
Tel : +86-21-5496-3311 Fax : +86-21-5496-0189

■ **FUJI ELECTRIC HOLDINGS CO., LTD.**
China Representative Office (Beijing)
CHINA
Tel : +86-10-6505-1263 Fax : +86-10-6505-1851

● **FUJI ELECTRIC FA (SHANGHAI) CO., LTD.**
CHINA
Tel : +86-21-5496-1177 Fax : +86-21-6422-4650

◆ **FUJI ELECTRIC (CHANGSHU) CO., LTD.**
CHINA
Tel : +86-512-5284-5642 Fax : +86-512-5284-5640

◆ **FUJI GE DRIVES (WUXI) CO., LTD.**
CHINA
Tel : +86-510-8815-2088 Fax : +86-510-8815-9159

◆ **FUJI ELECTRIC DALIAN CO., LTD.**
CHINA
Tel : +86-411-8762-2000 Fax : +86-411-8762-2030

◆ **SHANGHAI FUJI ELECTRIC SWITCHGEAR CO., LTD.**
CHINA
Tel : +86-21-5718-1495 Fax : +86-21-5718-5745

◆ **SHANGHAI FUJI ELECTRIC TRANSFORMER CO., LTD.**
CHINA
Tel : +86-21-5718-1495 Fax : +86-21-5718-5745

◆ **DALIAN FUJI BINGSHAN VENDING MACHINE CO., LTD.**
CHINA
Tel : +86-411-8730-5902 Fax : +86-411-8730-5911

● **DALIAN JIALE VENDING MACHINE OPERATION CO., LTD.**
CHINA
Tel : +86-411-8596-2730 Fax : +86-411-8596-2732

◆ **SHANGHAI GENERAL FUJI REFRIGERATION EQUIPMENT CO., LTD.**
CHINA
Tel : +86-21-6921-1088 Fax : +86-21-6921-1066

◆ **HANGZHOU FUJI REFRIGERATING MACHINE CO., LTD.**
CHINA
Tel : +86-571-8821-1661 Fax : +86-571-8821-0220

◆ **FUJI ELECTRIC (SHENZHEN) CO., LTD.**
CHINA
Tel : +86-755-2734-2910 Fax : +86-755-2734-2912

◆ **HONG KONG FUJIDENKI CO., LTD.**
HONG KONG
Tel : +852-2664-8699 Fax : +852-2664-8040

● **FUJI ELECTRIC FA (ASIA) CO., LTD.**
HONG KONG
Tel : +852-2311-8282 Fax : +852-2312-0566

● **FUJI ELECTRIC DEVICE TECHNOLOGY HONG KONG CO., LTD.**
HONG KONG
Tel : +852-2311-8282 Fax : +852-2312-0566

■ **FUJI ELECTRIC SYSTEMS CO., LTD.**
Taipei Representative Office
TAIWAN
Tel : +886-2-2561-1255 Fax : +886-2-2561-0528

● **FUJI ELECTRIC TAIWAN CO., LTD.**
TAIWAN
Tel : +886-2-2515-1850 Fax : +886-2-2515-1860

● **FUJI ELECTRIC FA TAIWAN CO., LTD.**
TAIWAN
Tel : +886-2-2556-0716 Fax : +886-2-2556-0717

◆ **ATAI FUJI ELECTRIC CO., LTD.**
TAIWAN
Tel : +886-3-321-3030 Fax : +886-3-321-7890

● **FUJI ELECTRIC FA KOREA CO., LTD.**
KOREA
Tel : +82-2-780-5011 Fax : +82-2-783-1707

Southeast Asia

■ **FUJI ELECTRIC SYSTEMS CO., LTD.**
Bangkok Representative Office
THAILAND
Tel : +66-2-308-2240, 2241 Fax : +66-2-308-2242

■ **FUJI ELECTRIC SYSTEMS CO., LTD.**
Jakarta Representative Office
INDONESIA
Tel : +62-21-572-4281 Fax : +62-21-572-4283

◆ **FUJI ELECTRIC (MALAYSIA) SDN. BHD.**
MALAYSIA
Tel : +60-4-403-1111 Fax : +60-4-403-1496

◆ **FUJI ELECTRIC PHILIPPINES, INC.**
PHILIPPINES
Tel : +63-2-844-6183 Fax : +63-2-844-6196

● **FUJI ELECTRIC SINGAPORE PRIVATE LTD.**
SINGAPORE
Tel : +65-6535-8998 Fax : +65-6532-6866

◆ **FUJI ELECTRIC FA SINGAPORE PRIVATE LTD.**
SINGAPORE
Tel : +65-6533-0010 Fax : +65-6533-0021

e-Front runners